Chapter 2
Multi-Terminal Network Elements

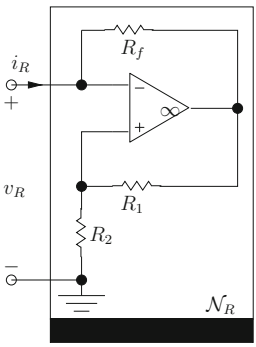

Two-terminal piecewise linear negative resistor, synthesized using a multi-terminal opamp

Abstract This chapter will naturally expand upon the ideas in Chap. 1 and discuss black boxes that have more than two terminals. We will first discuss characterization of a multi-terminal black box, followed by a discussion of the two-port representation technique. We will then talk about resistive, inductive (including transformers), and capacitive three-terminal elements. Circulators and opamps are next discussed. After this, we discuss the family of two-port scalors, rotators, reflectors, and gyrators. A current feedback opamp-based implementation approach is used for studying mutators.

2.1 Characterization of a Multi-Terminal Black Box

While the conventional resistor is probably the most familiar circuit element [6] [4], the transistor is certainly the electronic device that heralded the computer revolution. A transistor is a three-terminal device which behaves like a two-terminal nonlinear resistor when viewed from any pair of terminals, at low enough frequencies. This is

B. Muthuswamy, S. Banerjee, *Introduction to Nonlinear Circuits and Networks*,
https://doi.org/10.1007/978-3-319-67325-7_2

why its inventors (Nobel laureates Bardeen, Brattain, and Shockley) christened it as a **transfer resistor**, or transistor in brief.

The transistor is not the only multi-terminal device, many devices have more than two terminals. Our objective in this section is to learn how these multi-terminal devices may be characterized so that we shall be in a position to use them more effectively [3]. The basic principles discussed in the preceding chapter for characterizing two-terminal devices are still applicable. A set of measurable **independent** variables is selected and a series of external measurements are taken with the objective of deriving a consistent relationship among the variables. Once this relationship is found, we have characterized the black box because from then on, any design using this device can be undertaken on the basis of this relationship alone, thereby obviating the need for further measurements.

To discuss the selection of an independent set of variables, let us consider first the three-terminal black box shown in Fig. 2.1a. The most obvious variables are the currents i_1, i_2, and i_3 entering the terminals, and the voltages v_{12}, v_{23}, and v_{31} across the terminals. However, the black box in Fig. 2.1a can be enclosed by a Gaussian surface and hence the currents i_1, i_2, and i_3 entering this surface must satisfy KCL, namely, $i_1 + i_2 + i_3 = 0$.

Thus, if we know the value of any two of these currents, we can calculate the third, and therefore there is no need to measure all three currents. This observation is equivalent to saying that the three variables i_1, i_2, and i_3 are not independent. Similarly, from KVL we have $v_{12} + v_{23} + v_{31} = 0$ and hence the three variables v_{12}, v_{23}, and v_{31} are not independent.

Consequently, among the six variables shown in Fig. 2.1a, only two currents and two voltages are independent. For this reason, we may select any terminal to be ground and define the two currents i_1, i_2 and voltages v_1, v_2 as shown in Fig. 2.1b. In theory, there is no reason for preferring one terminal over another as the ground terminal. In practice, however, such a preference may be desirable

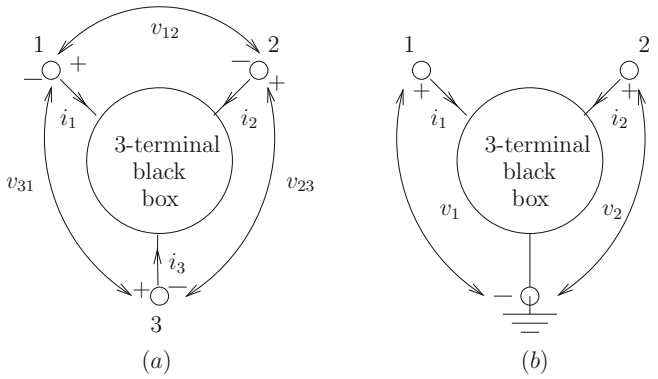

Fig. 2.1 In the process of characterizing a three-terminal black box, one terminal is arbitrarily chosen as the ground terminal. The voltages of the remaining terminals are measured with respect to the common terminal

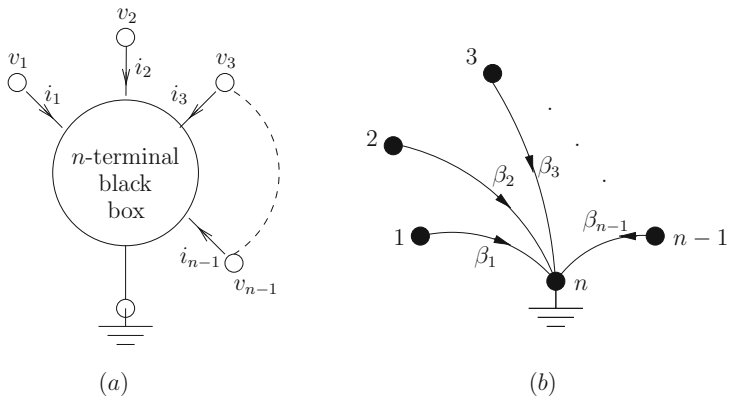

Fig. 2.2 For an n-terminal element, we can arbitrarily choose one terminal as ground. With n chosen as the ground terminal, we have the associated element graph

because the measurements may be easier and more accurately obtained.[1] To avoid ambiguity, it is of the utmost importance to specify the common terminal associated with the measured characteristics of a particular device. A ground terminal can also be arbitrarily chosen for a generic multi-terminal (or henceforth, n-terminal) element, as shown in Fig. 2.2a. Based on our choice of the ground terminal, we can also easily draw the associated element graph of the n-terminal device, as shown in Fig. 2.2b. Notice that we will have n possible element graphs for an n-terminal element, depending on our choice of the ground node.

With the abovementioned precaution of choosing the common terminal associated with the measured characteristic, let us investigate the type of measurements that may be taken. Just as in the two-terminal case, it is necessary to excite the black box by a voltage source or a current source. However, the response to these excitations need not be restricted to currents and voltages. Recall from Eq. (1.3) that it is possible to measure the charge q_j entering terminal j by integrating the current i_j, namely:

$$q_j(t) = \int_{-\infty}^{t} i_j(\tau) d\tau \quad j = 1, 2, \cdots, n-1 \tag{2.1}$$

Similarly, from Eq. (1.4), we can measure the flux-linkage ϕ_j associated with each voltage v_j between terminal j and ground by integrating the voltage v_j:

$$\phi_j(t) = \int_{-\infty}^{t} v_j(\tau) d\tau \quad j = 1, 2, \cdots, n-1 \tag{2.2}$$

[1] This is especially true for the transistor, where the characteristic curves can be more accurately, and more easily, measured if a particular terminal (called emitter for *npn* junction transistors) is chosen to be the ground terminal.

Hence, among the variables of interest to us are q_j, i_j, ϕ_j, and v_j ($j = 1, 2, \cdots, n-1$). Any **independent** combination of these variables constitute a valid set of measurements. Observe that the combination q_j and i_j (ϕ_j and v_j) is not valid because these variables are already related by Eqs. (2.1) and (2.2). If a certain set of measurements leads to some consistent relationship, then the device is said to be characterized by that relationship.

The corresponding element classifications now take the following forms:

1. n-terminal resistors, involving only $v_1, v_2, \cdots, v_{n-1}; i_1, i_2, \cdots, i_{n-1}$.
2. n-terminal inductors, involving only $i_1, i_2, \cdots, i_{n-1}; \phi_1, \phi_2, \cdots, \phi_{n-1}$.
3. n-terminal capacitors, involving only $v_1, v_2, \cdots, v_{n-1}; q_1, q_2, \cdots, q_{n-1}$.
4. n-terminal memristors, involving only $\phi_1, \phi_2, \cdots, \phi_{n-1}; q_1, q_2, \cdots, q_{n-1}$.

But, in general, in order to completely characterize an n-terminal black box, $n-1$ distinct laboratory setups are required. For example, Fig. 2.3 shows the setups necessary to characterize a four-terminal device.

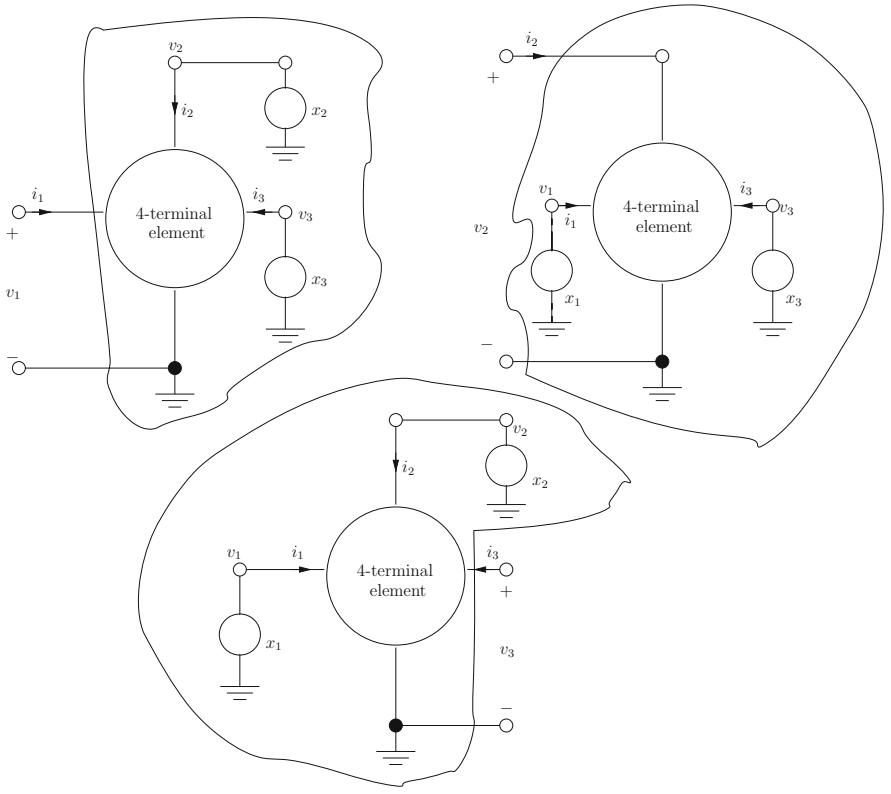

Fig. 2.3 To characterize a four-terminal black box, three distinct laboratory setups are required. Each setup involves as many sets of measurements as necessary to include all desired combinations of parameter values of the controlling variables

Thus, it is in general impractical to completely characterize an n-terminal black box when $n >> 3$. Fortunately, most practical devices have single digit values for n, and those devices will be discussed in the remainder of this chapter, starting with $n = 3$.

2.2 Three-Terminal Resistors, Inductors, and Capacitors

2.2.1 Two-Port Representation

The concept of a port was first introduced in Sect. 1.4. Recall that a port can be created from a circuit by connecting two leads to a pair of nodes of the circuit. Thus, a one-port can be viewed as a black box which has one pair of terminals from the outside. In the case of a multi-port such as the four-terminal black box from Fig. 2.3, we see that the box can be completely characterized with three sets of measurements, using three pairs of terminals.

As discussed previously, because of the complexity involved in practically characterizing a multi-terminal device for $n >> 3$ (n is the number of terminals), we will primarily discuss three-terminal elements or two-ports, with $n = 3$. For details on multi-ports, refer to section 4 from [6].

The generalization from a two-terminal to a three-terminal element amounts to extending from scalar port variables to $n - 1$-dimensional vector variables. For the purposes of clarity, we will discuss resistive two-ports in detail. For inductors, capacitors, and memristors, the principles are identical and hence for those elements, we will only discuss one form of representation.

A three-terminal element, or a two-port, will be called a (time-invariant) resistor if its port voltages and port currents satisfy the following relation:

$$\mathscr{R}_R = \{(v_1, v_2, i_1, i_2);\ f_1(v_1, v_2, i_1, i_2) = 0 \text{ and } f_2(v_1, v_2, i_1, i_2) = 0\} \tag{2.3}$$

This relation, similar to the two-terminal resistor given by Eq. (1.35) in Chap. 1, will be called **the $v - i$ characteristic of a three-terminal resistor or a resistive two-port**. The difference with respect to Eq. (1.35) is that we now need two scalar functions $f_1(\cdot)$ and $f_2(\cdot)$ to characterize a two-port and there are four scalar variables v_1, v_2, i_1, i_2. The characteristic is in general a two-dimensional surface in a four-dimensional space.

When we deal with two-ports, we often need to distinguish the ports, so one of them is marked as port 1 and the other is marked as port 2, as shown in Fig. 2.4. As a tradition, port 1 is often referred to as the **input port** and port 2 is often referred to as the **output port**.

We will now first consider linear resistors and use them to bring out pertinent concepts in the generalization from a two-terminal (one-port) to multi-terminal (two-port) element. Nonlinear two-ports such as transistors will be discussed in Sect. 2.2.2.

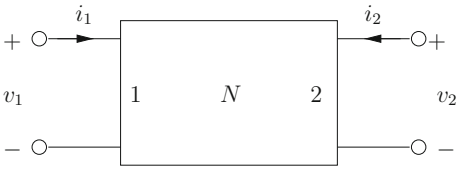

Fig. 2.4 A two-port with its port voltages v_1, v_2 and port currents i_1, i_2

Table 2.1 Six representations of a two-port

Representations	Dependent variables	Independent variables
Current-controlled	v_1, v_2	i_1, i_2
Voltage-controlled	i_1, i_2	v_1, v_2
Hybrid 1	v_1, i_2	i_1, v_2
Hybrid 2	i_1, v_2	v_1, i_2
Transmission 1	v_1, i_1	v_2, i_2
Transmission 2	v_2, i_2	v_1, i_1

Table 2.2 Equations for the six representations of a linear resistive two-port

Representations	Scalar equations	Vector equations
Current-controlled	$v_1 = r_{11}i_1 + r_{12}i_2$ $v_2 = r_{21}i_1 + r_{22}i_2$	$\mathbf{v} = \mathbf{R}\mathbf{i}$
Voltage-controlled	$i_1 = g_{11}v_1 + g_{12}v_2$ $i_2 = g_{21}v_1 + g_{22}v_2$	$\mathbf{i} = \mathbf{G}\mathbf{v}$
Hybrid 1	$v_1 = h_{11}i_1 + h_{12}v_2$ $i_2 = h_{21}i_1 + h_{22}v_2$	$\begin{bmatrix} v_1 \\ i_2 \end{bmatrix} = \mathbf{H} \begin{bmatrix} i_1 \\ v_2 \end{bmatrix}$
Hybrid 2	$i_1 = h'_{11}v_1 + h'_{12}i_2$ $v_2 = h'_{21}v_1 + h'_{22}i_2$	$\begin{bmatrix} i_1 \\ v_2 \end{bmatrix} = \mathbf{H}' \begin{bmatrix} v_1 \\ i_2 \end{bmatrix}$
Transmission 1	$v_1 = t_{11}v_2 - t_{12}i_2$ $i_1 = t_{21}v_2 - t_{22}i_2$	$\begin{bmatrix} v_1 \\ i_1 \end{bmatrix} = \mathbf{T} \begin{bmatrix} v_2 \\ -i_2 \end{bmatrix}$
Transmission 2	$v_2 = t'_{11}v_1 + t'_{12}i_1$ $-i_2 = t'_{21}v_1 + t'_{22}i_1$	$\begin{bmatrix} v_2 \\ i_2 \end{bmatrix} = \mathbf{T}' \begin{bmatrix} v_1 \\ i_1 \end{bmatrix}$

For the transmission representations, for historical reasons, a minus sign is used in conjunction with i_2. Because of the reference direction chosen for i_2, $-i_2$ gives the current leaving the output port

With four scalar variables v_1, v_2, i_1, i_2 and two equations to characterize a resistive two-port, there are $C_2^4 = 6$ possible two-port representations, since we may choose any two of the four variables as independent variables (the remaining two are then the dependent variables). Table 2.1 gives the classification of the six representations according to dependent and independent variables.

Table 2.2 gives the equations of the six possible representations of a linear resistive two-port.

In Table 2.2, $\mathbf{G}$ is the inverse matrix of $\mathbf{R}$. Similarly, we also have $\mathbf{H}' = \mathbf{H}^{-1}$ and $\mathbf{T}' = \mathbf{T}^{-1}$. We call $\mathbf{H}$ and $\mathbf{H}'$ hybrid matrices because both the dependent and independent variables are mixtures of a voltage and current. We call $\mathbf{T}$ and $\mathbf{T}'$ the transmission matrices because they relate the variables pertaining to one port to that pertaining to the other and the two-port serves as a transmission media. Hence, transmission matrices are important in the study of communication networks. A discussion of these networks is the beyond the scope of this book, but the interested reader is referred to Chapter 13 in [6].

Example 2.2.1 Consider a resistive two-port made up of three linear resistors as shown in Fig. 2.5. Determine the current-controlled and voltage-controlled representations.

Solution Let us apply two independent current sources to the two-port as shown in Fig. 2.6. KCL applied to nodes 1, 2, and 3 yields:

$$\begin{aligned} i_{s1} &= i_1 \\ i_{s2} &= i_2 \\ i_3 &= i_1 + i_2 \end{aligned} \tag{2.4}$$

Using Ohm's law and KVL for node sequences $1-3-4-1$ and $2-3-4-2$, we get:

$$\begin{aligned} v_1 &= i_1 R_1 + R_3(i_1 + i_2) = (R_1 + R_3)i_1 + R_3 i_2 \\ v_2 &= i_2 R_2 + R_3(i_1 + i_2) = R_3 i_1 + (R_2 + R_3)i_2 \end{aligned} \tag{2.5}$$

We will rewrite Eq. (2.5) in matrix form, to obtain the current-controlled representation from Table 2.2.

$$\begin{pmatrix} v_1 \\ v_2 \end{pmatrix} = \begin{pmatrix} R_1 + R_3 & R_3 \\ R_3 & R_2 + R_3 \end{pmatrix} \begin{pmatrix} i_1 \\ i_2 \end{pmatrix} \tag{2.6}$$

Hence, we have the resistance matrix $\mathbf{R}$ as defined in Eq. (2.7).

$$\mathbf{R} \triangleq \begin{pmatrix} R_1 + R_3 & R_3 \\ R_3 & R_2 + R_3 \end{pmatrix} \tag{2.7}$$

Notice that $\mathbf{R}$ is symmetrical: $\mathbf{R}^{\mathbf{T}} = \mathbf{R}$. Such symmetries will be exploited when we discuss resistive nonlinear networks in Chap. 3.

(continued)

Example 2.2.1 (continued)

Now, that we have **R**, **G** (conductance matrix) for the voltage-controlled representation is simply $\mathbf{R}^{-1}$:

$$\mathbf{G} \triangleq \mathbf{R}^{-1} = \frac{1}{R_1R_2 + R_2R_3 + R_3R_1} \begin{pmatrix} R_2 + R_3 & -R_3 \\ -R_3 & R_1 + R_3 \end{pmatrix} \tag{2.8}$$

In Example 2.2.1, we could have derived the voltage-controlled representation first by using independent voltage sources v_{s1} and v_{s2}, then used the fact that $\mathbf{R} \triangleq \mathbf{G}^{-1}$. In other words, it is quite simple to transform one two-port representation to another, as shown in Example 2.2.2.

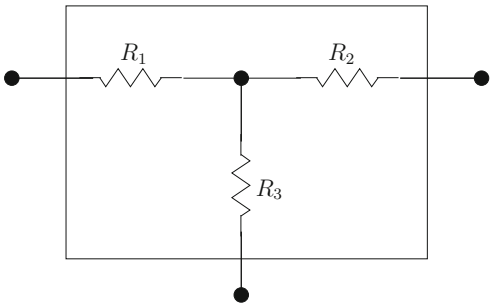

Fig. 2.5 The resistive T-network

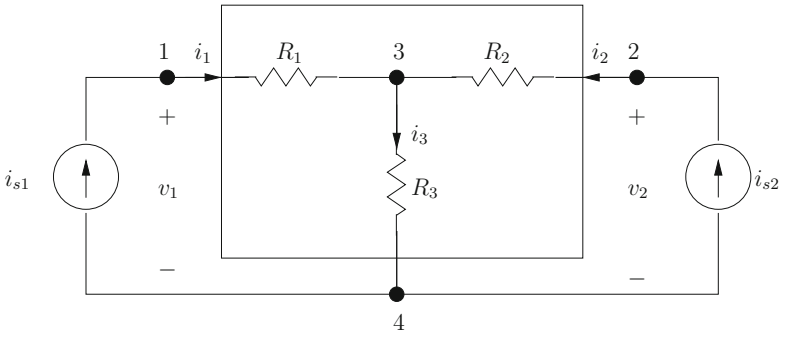

Fig. 2.6 For Example 2.2.1, we will use two independent current sources in Fig. 2.5 for obtaining the current-controlled representation

Example 2.2.2 In Example 2.2.1, let $R_1 = 1\ \Omega, R_2 = 2\ \Omega, R_3 = 3\ \Omega$. Determine the numerical current-controlled representation and the other representations from Table 2.2.

Solution The numerical current-controlled representation is given by Eq. (2.6):

$$\begin{pmatrix} v_1 \\ v_2 \end{pmatrix} = \begin{pmatrix} 4 & 3 \\ 3 & 5 \end{pmatrix} \begin{pmatrix} i_1 \\ i_2 \end{pmatrix} \tag{2.9}$$

The voltage-controlled representation can be found using $\mathbf{G}$ in Eq. (2.8) or by inverting the numerical square matrix in Eq. (2.9):

$$\begin{pmatrix} i_1 \\ i_2 \end{pmatrix} = \begin{pmatrix} \frac{5}{11} & \frac{-3}{11} \\ \frac{-3}{11} & \frac{4}{11} \end{pmatrix} \begin{pmatrix} v_1 \\ v_2 \end{pmatrix} \tag{2.10}$$

It is straightforward to derive the other four representations from the equations above. The general treatment is beyond the scope of this book but can be found in classic references such as [6]. However, it is easy to obtain, for example, the hybrid representations.

For the Hybrid 2 representation, we first solve for i_1 in terms of v_1 and i_2 by using the first row from Eq. (2.9). Next, we solve for v_2 in terms of v_1 and i_2 by using the second row from Eq. (2.10). Thus:

$$\begin{pmatrix} i_1 \\ v_2 \end{pmatrix} = \begin{pmatrix} \frac{1}{4} & \frac{-3}{4} \\ \frac{3}{4} & \frac{11}{4} \end{pmatrix} \begin{pmatrix} v_1 \\ i_2 \end{pmatrix} \tag{2.11}$$

The hybrid 1 representation can be found by inverting $\mathbf{H}'$ from Eq. (2.11):

$$\mathbf{H} = \begin{pmatrix} \frac{11}{5} & \frac{3}{5} \\ \frac{-3}{5} & \frac{1}{5} \end{pmatrix} \tag{2.12}$$

The transmission matrices can be obtained in a similar manner and is left as an exercise for the reader.

2.2.1.1 Physical Interpretations

In the examples from Sect. 2.2.1, we derived various two-port representations. In particular, we derived the current-controlled representation by using two current sources at the two-ports and determining the two-port voltages (as shown in Fig. 2.6).

For a physical interpretation of two-ports, recall from Chap. 1 that we defined a linear two-terminal resistor as one having a straight line characteristic passing through the origin in the $v - i$ plane. For two-ports, we have four variables and two equations, e.g., the current-controlled representation is:

$$\begin{aligned} v_1 &= r_{11} i_1 + r_{12} i_2 \\ v_2 &= r_{21} i_1 + r_{22} i_2 \end{aligned} \tag{2.13}$$

These two equations impose two linear constraints on the port voltages and the port currents and hence the point representing the four variables; namely, (v_1, v_2, i_1, i_2) is constrained to a two-dimensional subspace in the four-dimensional space spanned by v_1, v_2, i_1, i_2. Of course, this is difficult to visualize. However, if we take one equation at a time, we can represent it by a family of curves in the appropriate $i - v$ planes, as shown in Fig. 2.7.

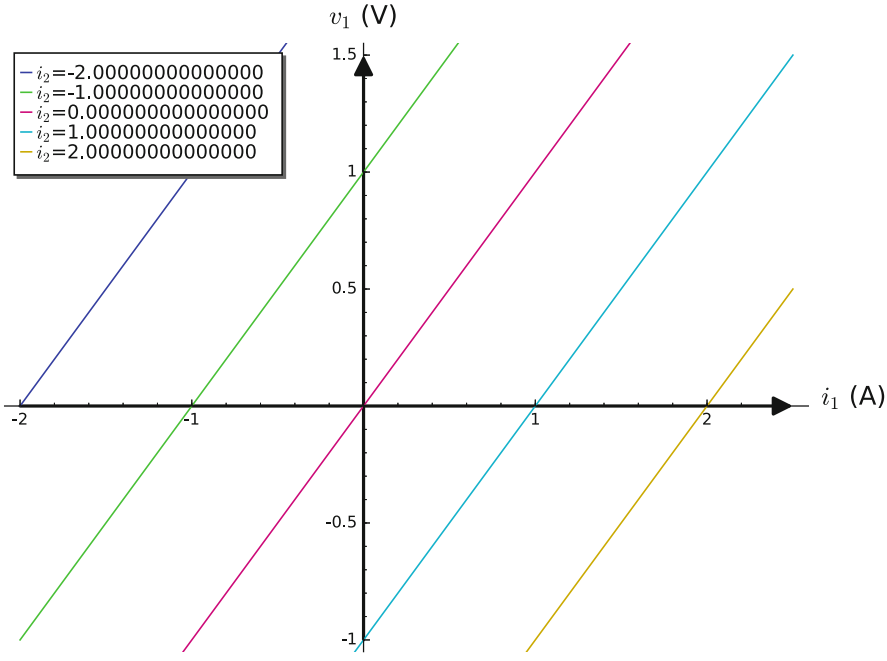

Fig. 2.7 Two-port characteristics plotted on the $i_1 - v_1$ plane, with i_2 as parameter. $r_{11} = 1, r_{12} = -1$. A similar plot can be generated for $i_2 - v_2$ plane

From the first equation in Eq. (2.13), we can give the following interpretations for r_{11} and r_{12}:

$$r_{11} = \left.\frac{v_1}{i_1}\right|_{i_2=0} \tag{2.14}$$

Thus, r_{11} is called the **driving-point resistance at port 1** when $i_2 = 0$, i.e., port 2 is kept open circuited. Similarly, r_{12} can be interpreted by:

$$r_{12} = \left.\frac{v_1}{i_2}\right|_{i_1=0} \tag{2.15}$$

Hence, r_{12} is called the **transfer resistance when** $i_1 = 0$, i.e., port 1 is kept open circuited.

Analogously, we can derive the following relationships from the second equation in Eq. (2.13):

$$r_{21} = \left.\frac{v_2}{i_1}\right|_{i_2=0} \tag{2.16}$$

$$r_{22} = \left.\frac{v_2}{i_2}\right|_{i_1=0} \tag{2.17}$$

r_{21} is the **transfer resistance when** $i_2 = 0$ and r_{22} is the **driving-point resistance at port 2**. Figure 2.8 gives the physical interpretations of Eq. (2.14) through (2.17).

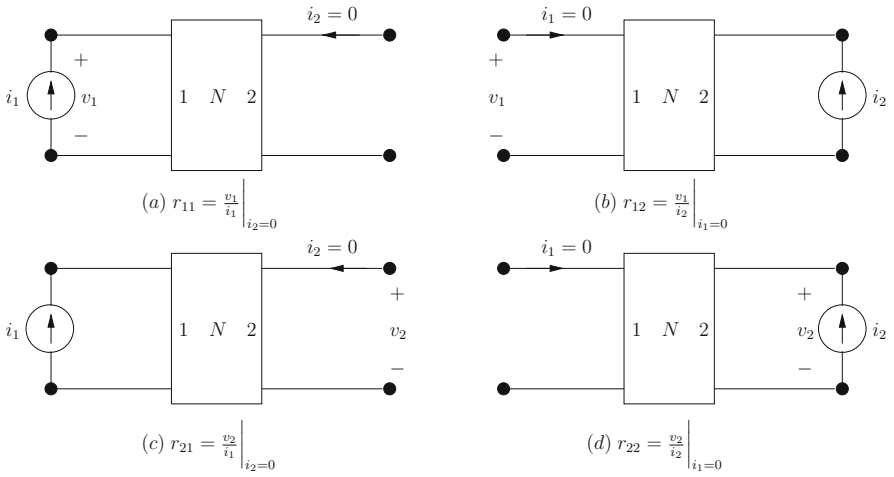

Fig. 2.8 Interpretations of (**a**) r_{11}, (**b**) r_{12}, (**c**) r_{21}, and (**d**) r_{22}

Example 2.2.3 Give the physical interpretation of the hybrid 1 linear resistive two-port representation from Table 2.2.

Solution The two equations for the hybrid 1 representation read:

$$v_1 = h_{11} i_1 + h_{12} v_2 \tag{2.18}$$

$$i_2 = h_{21} i_1 + h_{22} i_2 \tag{2.19}$$

Following the same treatment as the current-controlled representation, we write:

$$h_{11} = \left.\frac{v_1}{i_1}\right|_{v_2=0} \tag{2.20}$$

$$h_{12} = \left.\frac{v_1}{v_2}\right|_{i_1=0} \tag{2.21}$$

$$h_{21} = \left.\frac{i_2}{i_1}\right|_{v_2=0} \tag{2.22}$$

$$h_{22} = \left.\frac{i_2}{v_2}\right|_{i_1=0} \tag{2.23}$$

The physical interpretations of the sources, responses, and external connections for the four hybrid representations are shown in Fig. 2.9.

Note that the four hybrid parameters $h_{11}, h_{12}, h_{21}, h_{22}$ represent a **driving-point resistance**, **a reverse voltage transfer ratio**, **a forward current transfer ratio**, and a **driving-point conductance**, respectively. As we will see in Sect. 3.1, the hybrid representation is obtained when we derive the small-signal model for the common-emitter configuration of the bipolar junction transistor.

Analogous interpretations can be given for other two-port representations such as the current-controlled representation.

2.2.1.2 Dependent Sources

Up to this point, we have encountered independent voltage and current sources. Independent sources are used as inputs to a circuit. In this section, we will introduce another type of source, called **controlled sources** or **dependent sources**.

A controlled source is a resistive two-port element consisting of two branches: a primary branch which is either an open circuit or a short circuit and a secondary branch which is either a voltage source or a current source. The voltage or current waveform in the secondary branch is **controlled** by (or **dependent** upon) the

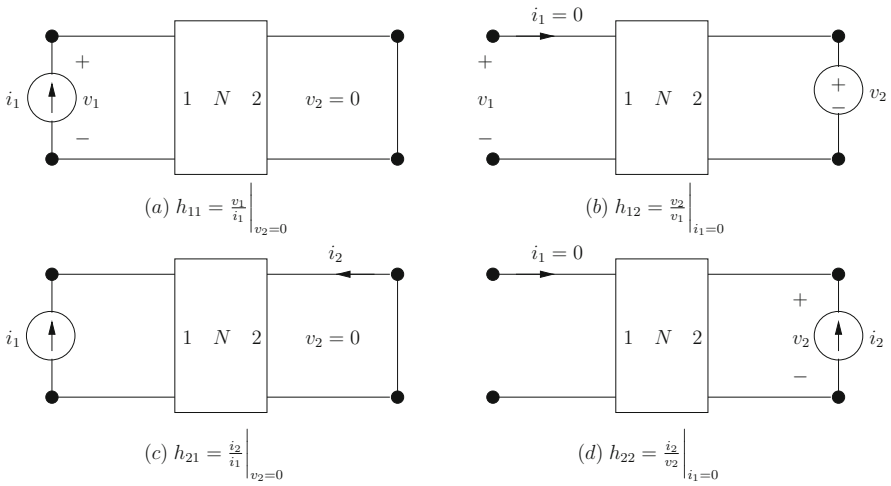

Fig. 2.9 Interpretations of (**a**) h_{11}, (**b**) h_{12}, (**c**) h_{21}, and (**d**) h_{22}

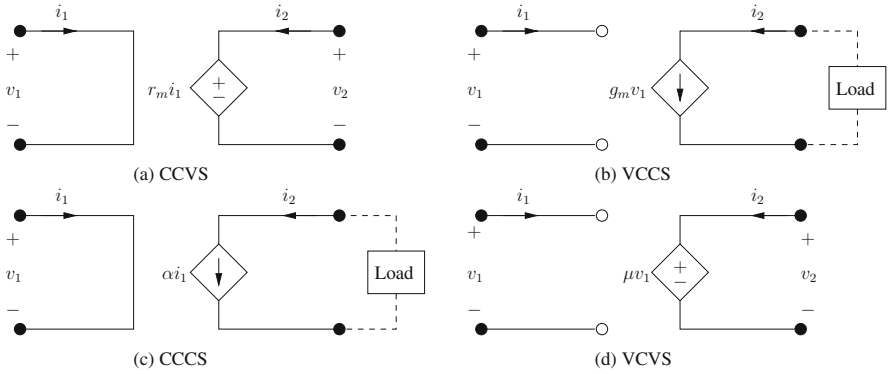

Fig. 2.10 Four types of linear controlled sources

voltage or current of the primary branch. Therefore, there exist four types of controlled sources depending on whether the primary branch is an open circuit or a short circuit and whether the secondary branch is a voltage source or a current source. The four types of controlled sources are shown in Fig. 2.10. They are the **current-controlled voltage source** (CCVS), **voltage-controlled current source** (VCCS), **current-controlled current source** (CCCS), and **voltage-controlled current source** (VCCS). Note that we use a **diamond-shaped**[2] symbol to denote controlled sources. This is to differentiate them from the independent sources.

[2]Diamond-shaped symbol for controlled sources was used for the first time in [3].

Each linear controlled source is characterized by two linear equations:

$$\text{CCVS:} \qquad v_1 = 0 \qquad v_2 = r_m i_1 \tag{2.24}$$

$$\text{VCCS:} \qquad i_1 = 0 \qquad i_2 = g_m v_1 \tag{2.25}$$

$$\text{CCCS:} \qquad v_1 = 0 \qquad i_2 = \alpha i_1 \tag{2.26}$$

$$\text{VCVS:} \qquad i_1 = 0 \qquad v_2 = \mu v_1 \tag{2.27}$$

r_m is the **transresistance**, g_m is the **transconductance**, α is called the **current transfer ratio**, and μ is called the **voltage transfer ratio**. They are all constants, thus the four controlled sources are linear time-invariant two-port resistors. More generally, if a CCVS is characterized by the two equations: $v_1 = 0, v_2 = f(i_1)$, where $f(\cdot)$ is a given **nonlinear** function, then that CCVS is a **nonlinear controlled source**. Similarly, if a CCCS is characterized by the two equations $v_1 = 0, i_2 = \alpha(t) i_1$, where $\alpha(\cdot)$ is a given function of time, then this CCCS is a **linear time-varying controlled source**.

Recall from Table 2.2, a linear resistive two-port has six representations. In the case of linear controlled sources, Eq. (2.24) to (2.27) can be put in matrix form for each corresponding to one representation:

$$\text{CCVS:} \qquad \begin{pmatrix} v_1 \\ v_2 \end{pmatrix} = \begin{pmatrix} 0 & 0 \\ r_m & 0 \end{pmatrix} \begin{pmatrix} i_1 \\ i_2 \end{pmatrix} \tag{2.28}$$

$$\text{VCCS:} \qquad \begin{pmatrix} i_1 \\ i_2 \end{pmatrix} = \begin{pmatrix} 0 & 0 \\ g_m & 0 \end{pmatrix} \begin{pmatrix} v_1 \\ v_2 \end{pmatrix} \tag{2.29}$$

$$\text{CCCS:} \qquad \begin{pmatrix} v_1 \\ i_2 \end{pmatrix} = \begin{pmatrix} 0 & 0 \\ \alpha & 0 \end{pmatrix} \begin{pmatrix} i_1 \\ v_2 \end{pmatrix} \tag{2.30}$$

$$\text{VCVS:} \qquad \begin{pmatrix} i_1 \\ v_2 \end{pmatrix} = \begin{pmatrix} 0 & 0 \\ \mu & 0 \end{pmatrix} \begin{pmatrix} v_1 \\ i_2 \end{pmatrix} \tag{2.31}$$

In Eq. (2.28), we have the current-controlled representation for the CCVS. Since the resistance matrix is singular, its inverse does not exist. Therefore, there is no voltage-controlled representation for a CCVS. In fact, it is easy to see that neither of the hybrid representations exists as well. We can make similar statements for the other three controlled sources, i.e., only one of the representations in the first four rows of Table 2.2 exists.

Linear controlled sources are extremely useful in modeling electronic devices and circuits, as we will see in Sect. 2.2.2. In Sect. 2.5.2.1, we will see that all four controlled sources can be realized physically (to a good approximation) by using operational amplifiers.

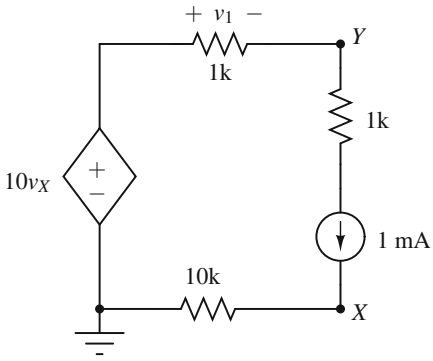

Fig. 2.11 Figure for Example 2.2.4

Example 2.2.4 In Fig. 2.11, determine the values of v_X and v_Y.

Solution We have a VCVS, whose input depends on v_X (voltage at node X with respect to ground). To avoid clutter, we have not explicitly drawn the two-port form for the VCVS. But, the reader **must** understand that all dependent sources are two-ports.

Since all elements in the circuit are in series, the current flowing through all elements is 1 mA, due to the constant current source. Since all resistors are also linear, by Ohm's law and the passive sign convention, we have:

$$\begin{aligned} v_X &= 1 \cdot 10 \text{ V} \\ &= 10 \text{ V} \end{aligned} \tag{2.32}$$

From KVL:

$$v_Y + v_1 - 10v_X = 0 \tag{2.33}$$

Hence:

$$\begin{aligned} v_Y &= 10v_X - v_1 \\ &= 99 \text{ V} \end{aligned} \tag{2.34}$$

2.2.1.3 Transformers

The **ideal transformer** is an ideal two-port resistive circuit element which is characterized by the following two equations:

$$v_1 = nv_2 \tag{2.35}$$

$$i_2 = -ni_1 \tag{2.36}$$

where n is a real number called the **turns ratio**. The symbol for the ideal transformer is shown in Fig. 2.12.

The ideal transformer is a **linear** resistive two-port, since its equations impose **linear** constraints on its port voltages and port currents. Note that neither the current-controlled representation nor the voltage-controlled representation exists for the ideal transformer. Eqs. (2.35) and (2.35) can be written in matrix form in terms of the hybrid matrix representation:

$$\begin{pmatrix} v_1 \\ i_2 \end{pmatrix} = \mathbf{H} \begin{pmatrix} i_1 \\ v_2 \end{pmatrix} = \begin{pmatrix} 0 & n \\ -n & 0 \end{pmatrix} \begin{pmatrix} i_1 \\ v_2 \end{pmatrix} \tag{2.37}$$

The ideal transformer is an idealization of a physical transformer, constructed using coupled inductors, that is used in many applications. The properties of the physical transformer will be discussed in Sect. 2.2.3.

We wish to stress that because the ideal transformer is an ideal element defined by Eq. (2.37), the relation between port voltages and port currents holds for all waveforms and for all frequencies, including DC.

Two fundamental properties of the ideal transformer are:

1. The ideal transformer neither dissipates nor stores energy. Indeed, the power entering the two-port at time t from Eq. (2.37) is:

$$p(t) = v_1(t)i_1(t) + v_2(t)i_2(t) = 0 \tag{2.38}$$

Thus, the ideal transformer is a **non-energic** element (another non-energic element is the ideal diode).

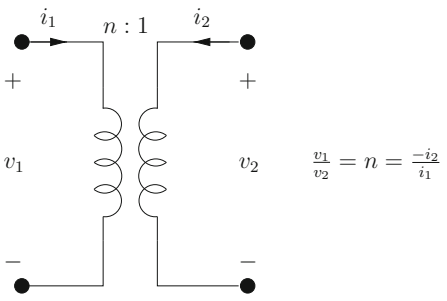

Fig. 2.12 An ideal transformer defined by the single parameter n, the turns ratio. Notice that the sign of i_2 is negative in the expression for n, confirming to the passive sign convention

2. When the ideal transformer is terminated at the output port with an $R-\Omega$ resistor, the input port behaves as a linear resistor with resistance n^2R. In other words:

$$v_2 = -i_2 R \tag{2.39}$$

Therefore, $\frac{v_1}{i_1} = \frac{nv_2}{-i_2/n} = n^2 R$.

2.2.2 *Three-Terminal Resistors*

In the previous sections, we discussed linear resistive two-ports and their various characterizations and properties. In the real world, we need to deal with **nonlinear** resistive two-ports and three-terminal devices, such as transistors. Much of the material given in the previous two sections can be extended and generalized to the nonlinear case. For brevity, we will simply summarize the six nonlinear representations in Table 2.3.

2.2.2.1 The npn Bipolar Transistor

Perhaps, the most commonly used three-terminal nonlinear resistor is a transistor. These devices come in mainly two variants—the bipolar junction transistor (BJT) and the metal-oxide-semiconductor field-effect transistor (MOSFET). We will discuss the low-frequency characteristics of the *npn* BJT here, together with some aspects of modeling. A discussion of MOSFETs can be found in excellent texts such as [7].

Consider the common-base *npn* transistor as shown in Fig. 2.13. The nodes are labeled e, b, and c corresponding to the emitter, base, and collector, respectively.

Table 2.3 Equations for the six representations of a nonlinear resistive two-port

Representations	Scalar equations
Current-controlled	$v_1 = \hat{v}_1(i_1, i_2)$ $v_2 = \hat{v}_2(i_1, i_2)$
Voltage-controlled	$i_1 = \hat{i}_1(v_1, v_2)$ $i_2 = \hat{i}_2(v_1, v_2)$
Hybrid 1	$v_1 = \hat{v}_1(i_1, v_2)$ $i_2 = \hat{i}_2(i_1, v_2)$
Hybrid 2	$i_1 = \hat{i}_1(v_1, i_2)$ $v_2 = \hat{v}_2(v_1, i_2)$
Transmission 1	$v_1 = \hat{v}_1(v_2, -i_2)$ $i_1 = \hat{i}_1(v_2, -i_2)$
Transmission 2	$v_2 = \hat{v}_2(v_1, i_1)$ $-i_2 = \hat{i}_2(v_1, i_1)$

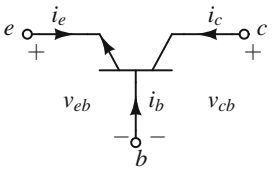

Fig. 2.13 The common-base *npn* transistor

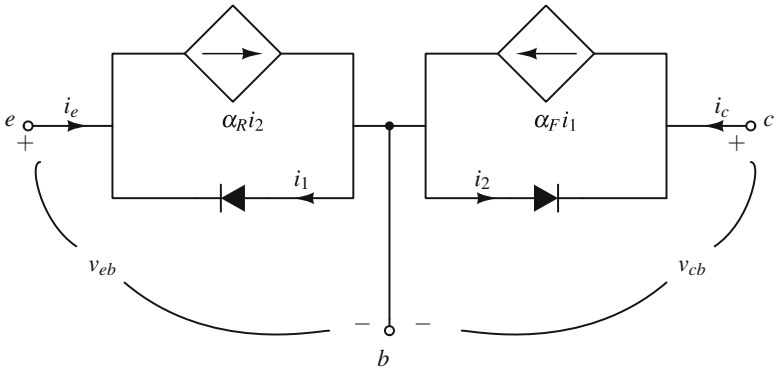

Fig. 2.14 Ebers–Moll circuit model of *npn* transistor

A good low-frequency characterization is given by the one-dimensional diffusion model which yields the **Ebers–Moll** equations:

$$i_e = -I_{ES}\left(e^{\frac{-v_{eb}}{V_T}} - 1\right) + \alpha_R I_{CS}\left(e^{\frac{-v_{cb}}{V_T}} - 1\right) \tag{2.40}$$

$$i_c = \alpha_F I_{ES}\left(e^{\frac{-v_{eb}}{V_T}} - 1\right) - I_{CS}\left(e^{\frac{-v_{cb}}{V_T}} - 1\right) \tag{2.41}$$

I_{ES}, I_{CS}, α_R, and α_F are device parameters. V_T is the thermal voltage defined earlier in Sect. 1.9.1, where we discussed the diode. Typically, $\alpha_R = 0.5$–0.8, $\alpha_F = 0.99$; I_{ES}, I_{CS} are on the order of 10^{-12} to 10^{-10} at 25°C. $V_T \approx 26$ mV at 25°C. Note that an *npn* BJT is in essence two **interacting** *pn*-junction diodes connected back to back to form a three-terminal device. Thus, with the base terminal as the ground node, the currents i_e and i_c entering the device at the emitter and the collector, respectively, are functions of two node-to-ground voltages v_{eb} and v_{cb}. From Eqs. (2.40) and (2.41), we see that the transistor is a **three-terminal voltage-controlled nonlinear resistor**. It can be represented by the equivalent circuit in Fig. 2.14, where the two *pn*-junctions are connected at the base node b to model the terms $-I_{ES}\left(e^{\frac{-v_{eb}}{V_T}} - 1\right)$ and $-I_{CS}\left(e^{\frac{-v_{cb}}{V_T}} - 1\right)$. The two CCCS are used to

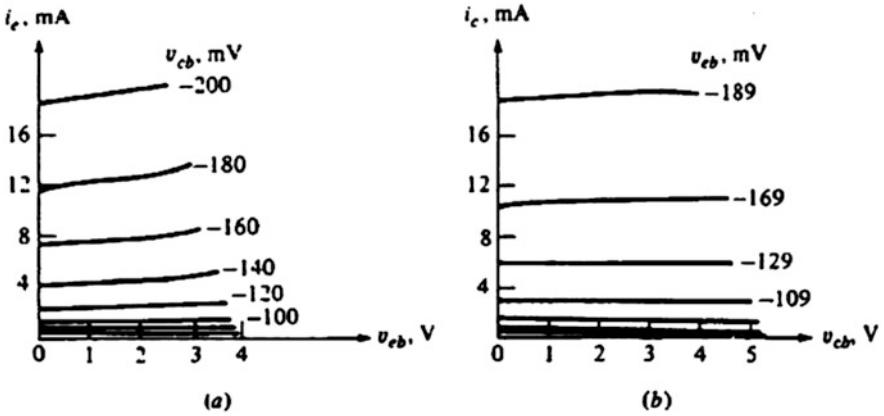

Fig. 2.15 Characteristics of an *npn* BJT in the common-base configuration [6]

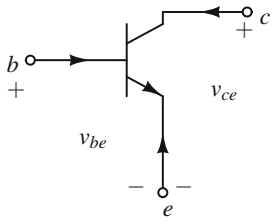

Fig. 2.16 The common-emitter *npn* transistor

model the terms $\alpha_R I_{CS}\left(e^{\frac{-v_{cb}}{V_T}}-1\right)$ and $\alpha_F I_{ES}\left(e^{\frac{-v_{eb}}{V_T}}-1\right)$ which represent the interaction between the two diodes.

The characteristics of Eqs. (2.40) and (2.41) are shown in Fig. 2.15 in the $v_{eb}-i_e$ plane and the $v_{cb}-i_c$ plane, respectively. Note that v_{cb} serves as a parameter in the family of curves in the $v_{eb}-i_e$ plane. Similarly, v_{eb} serves as a parameter in the family of curves in the $v_{cb}-i_c$ plane.

In most amplifier circuits, the common-emitter configuration shown in Fig. 2.16 is used. It is possible to derive equations for the common-emitter configuration directly from those of the common-base configuration of Eqs. (2.40) and (2.41). For the common-emitter configuration, the two-port voltages are v_{be} and v_{ce}. The two-port currents are i_b and i_c. These can be related to the variables of the common-base configuration by simply using Kirchhoff's laws:

$$v_{be} = -v_{eb} \tag{2.42}$$

$$v_{ce} = v_{cb} - v_{eb} \tag{2.43}$$

$$i_b = -(i_e + i_c) \tag{2.44}$$

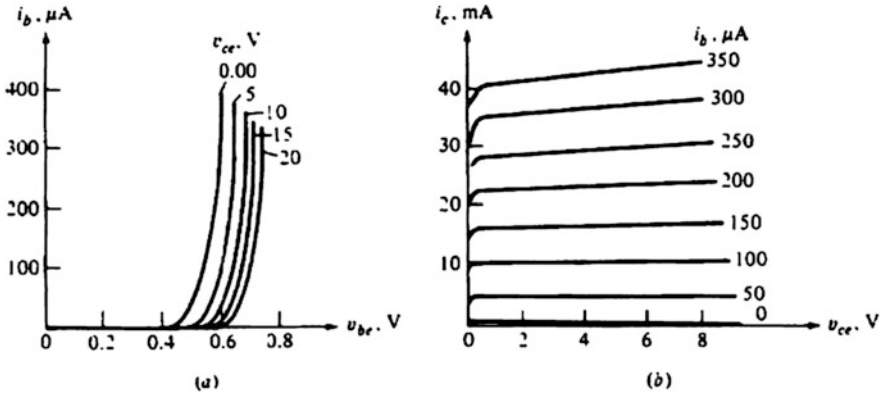

Fig. 2.17 Characteristics of an *npn* BJT in the common-emitter configuration [6]

Substituting the above equations into Eqs. (2.40) and (2.41), we can express the port currents i_b and i_c for the common-emitter configuration in terms of the port voltages v_{be} and v_{ce}. They are:

$$i_b = (1-\alpha_F) I_{ES}\left(e^{\frac{v_{be}}{V_T}} - 1\right) + (1-\alpha_R) I_{CS}\left(e^{\frac{v_{be}-v_{ce}}{V_T}} - 1\right) \tag{2.45}$$

$$i_c = \alpha_F I_{ES}\left(e^{\frac{v_{be}}{V_T}} - 1\right) - I_{CS}\left(e^{\frac{v_{be}-v_{ce}}{V_T}} - 1\right) \tag{2.46}$$

Thus, we again have a voltage-controlled representation for the common-emitter configuration. This set of equations is not particularly useful, because in practice, the measured data are usually expressed in terms of the hybrid 1 representation, i.e.,

$$v_{be} = \hat{v}_{be}(i_b, v_{ce}) \tag{2.47}$$

$$i_c = \hat{i}_c(i_b, v_{ce}) \tag{2.48}$$

Furthermore, as a tradition, we usually plot i_b vs v_{be} with v_{ce} as a parameter, and i_c vs v_{ce} with i_b as a parameter, as shown in Fig. 2.17. This is because we get a smoothly varying family of collector-to-emitter $v-i$ curves.

2.2.2.2 BJT Piecewise-Linear Approximation

As stated earlier, we often rely on measured data for characterizing physical (particularly nonlinear) electronic devices, such as the transistor. We will use the PWL approximation from Sect. 1.9.1.2, which will help us obtain circuit models, given the characteristic curves provided by device manufacturers in respective **datasheets** of their devices. The PWL characteristics of an *npn* BJT are shown in

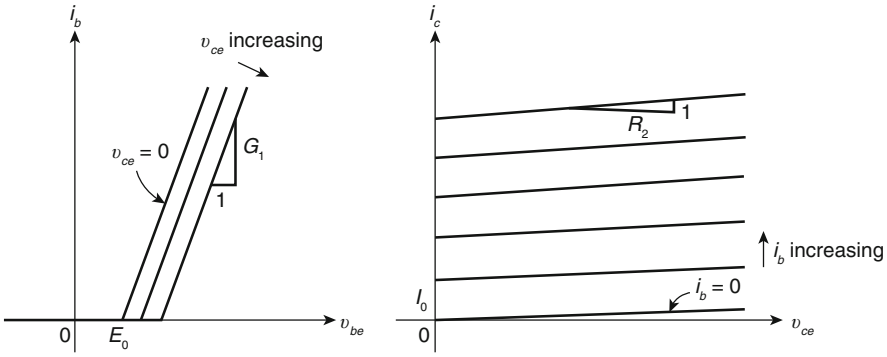

Fig. 2.18 PWL approximation of common-emitter characteristics [6]

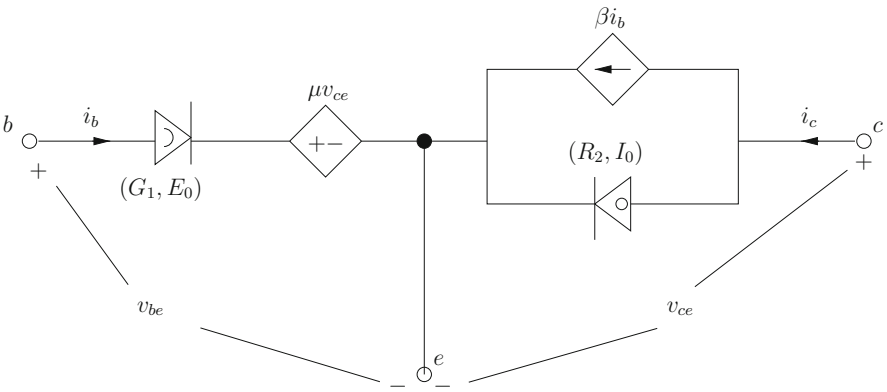

Fig. 2.19 PWL model of common-emitter BJT configuration

Fig. 2.18. The equivalent circuit for this representation is shown in Fig. 2.19. Note that with $v_{ce} = 0$, the $v_{be} - i_b$ characteristic in Fig. 2.18 is precisely that of a concave resistor specified by E_0 and slope G_1. In Fig. 2.19, we can see that if $v_{ce} = 0$, we simply have a concave resistor across the base-emitter terminal. In Fig. 2.18, the $v_{be} - i_b$ characteristic shifts to the right as v_{ce} increases. This is modeled in Fig. 2.19 by a VCVS with transfer voltage ratio μ.

Similarly, in the $v_{ce} - i_c$ characteristic in Fig. 2.18, with $i_b = 0$ the characteristic is of a convex resistor with i_c-axis intercept equal to I_0 and the slope equal to $\frac{1}{R}$. As i_b increases, the current i_c increases. These behaviors are modeled using a convex resistor and CCCS in Fig. 2.19, respectively.

For many large-signal applications, example H-bridges that simply run DC motors forward or backwards, these models are unnecessarily complicated and further simplifications are possible. But, it is important to again (recall Sect. 1.7) bear in mind that models are developed with specific applications in mind. Obviously, the simpler the model, the easier the circuit analysis. Thus, for applications where only

an approximate solution is called for, we should use the simplest but valid model to get an idea of how the circuit functions. In other situations, example in determining the precise operating points using a computer, we need to use a more precise model for the transistor than that of the Ebers–Moll model. A variety of such models exist and are implemented by programs such as QUCS and SPICE. We will not cover such models in this book.

2.2.3 Three-Terminal Inductors

A three-terminal element is called a **three-terminal inductor** if it can be characterized by two sets of curves, or relationships, involving the variables i_1, i_2, ϕ_1, ϕ_2. Just as for three-terminal resistors, there are several possible forms of representation. Since the principles are identical, only one form will be discussed here, namely:

$$\phi_1 = \phi_1(i_1, i_2) \tag{2.49}$$

$$\phi_2 = \phi_2(i_1, i_2) \tag{2.50}$$

To find the voltages v_1 and v_2 corresponding to any current waveforms i_1 and i_2, we apply the chain rule, thereby obtaining:

$$v_1(t) = \frac{\partial \phi_1}{\partial i_1}\frac{di_1}{dt} + \frac{\partial \phi_1}{\partial i_2}\frac{di_2}{dt} \tag{2.51}$$

$$v_2(t) = \frac{\partial \phi_2}{\partial i_1}\frac{di_1}{dt} + \frac{\partial \phi_2}{\partial i_2}\frac{di_2}{dt} \tag{2.52}$$

Practically speaking, we will only discuss linear three-terminal inductors. Hence, Eqs. (2.51) and (2.52) reduce to:

$$v_1(t) = L_{11}\frac{di_1}{dt} + L_{12}\frac{di_2}{dt} \tag{2.53}$$

$$v_2(t) = L_{21}\frac{di_1}{dt} + L_{22}\frac{di_2}{dt} \tag{2.54}$$

The reason for discussing only linear three-terminal inductors is that the most common type of commercially available three-terminal inductor is that of a toroidal coil with a center tap, which is precisely a **physical transformer** (or transformers). These devices are of crucial importance in power circuitry and are hence discussed in a separate subsection below.

2.2.3.1 Physical Transformers

A transformer that implements Eqs. (2.53) and (2.54) is shown in Fig. 2.20. The ferromagnetic material used for the torus in Fig. 2.20 is typically ferrite or thin sheets of special steel. As shown in Fig. 2.20, we have wound on this torus two coils; we thus obtain a two-port. If we drive the first port with a generator so that the current i_1 is positive and have the second port open (hence $i_2 = 0$), there will be a strong magnetic field setup in the torus, **H** as indicated in the figure. Note if i_1 varies with time, since the magnetic field links the second coil, there will be a time-varying flux through that second coil. Hence, by Faraday's law, a voltage will be induced and $v_2(t) \neq 0$. Thus, electrical energy is transferred between the two-ports via electromagnetic induction.

Referring back to Eqs. (2.53) and (2.54), from fundamental energy considerations in physics, $L_{12} = L_{21} = M$, where M is the **mutual inductance** of inductor 1 and inductor 2. We know from our discussion of the two-terminal inductor in Sect. 1.9.3, L_{11} is the **self-inductance** of inductor 1 and L_{22} is the self-inductance of inductor 2. The schematic symbol for coupled coils is shown in Fig. 2.21. Note that we can rewrite Eqs. (2.53) and (2.54) in matrix form:

$$\begin{pmatrix} v_1 \\ v_2 \end{pmatrix} = \begin{pmatrix} L_{11} & M \\ M & L_{22} \end{pmatrix} \begin{pmatrix} \dot{i}_1 \\ \dot{i}_2 \end{pmatrix} \tag{2.55}$$

The square matrix L in Eq. (2.55) is called the **inductance matrix**. There is a very important relationship between a physical transformer and the ideal transformer discussed in Sect. 2.2.1.3, as Example 2.2.5 shows.

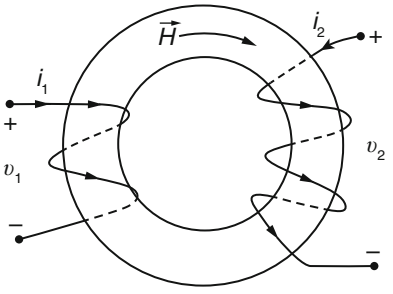

Fig. 2.20 Two coupled coils wound on a torus of ferromagnetic material

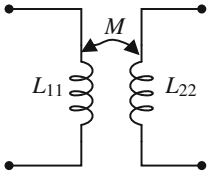

Fig. 2.21 Schematic symbol used for coupled coils with mutual inductance M, with self-inductances L_{11}, L_{22}

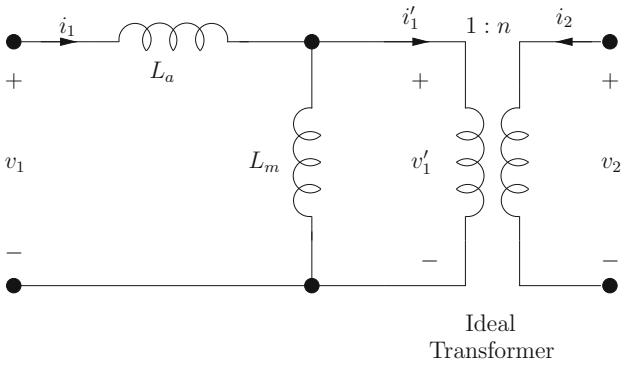

Fig. 2.22 A two-port equivalent to a pair of coupled inductors

Example 2.2.5 Show that Fig. 2.22, a two-port made up of an ideal transformer and two (uncoupled) inductors L_a and L_m, is equivalent to a pair of linear time-invariant coupled inductors modeled by Eq. (2.55).

Solution We will need to derive a form of Eq. (2.55) from Fig. 2.22. First, notice that for the ideal transformer, we have the following:

$$v_1' = \frac{1}{n} v_2 \tag{2.56}$$

$$i_2 = \frac{-1}{n} i_1' \tag{2.57}$$

Using the $v - i$ relationship for a two-terminal inductor and applying KCL to the node between L_a and L_m, we get:

$$v_1(t) = L_a \frac{di_1}{dt} + L_m \frac{d(i_1 - i_1')}{dt} \tag{2.58}$$

Hence, we have:

$$v_1(t) = (L_a + L_m) \frac{di_1}{dt} - L_m \frac{di_1'}{dt} \tag{2.59}$$

Substituting for i_1' from Eq. (2.57), we get:

$$v_1(t) = (L_a + L_m) \frac{di_1}{dt} + nL_m \frac{di_2}{dt} \tag{2.60}$$

(continued)

Example 2.2.5 (continued)
Using Eq. (2.56), we get:

$$v_2 = nv_1' \tag{2.61}$$

But, from Fig. 2.22, we get:

$$v_1' = L_m \frac{di_1 - i_1'}{dt} \tag{2.62}$$

Thus:

$$v_2 = nL_m \frac{di_1}{dt} - nL_m \frac{di_1'}{dt} \tag{2.63}$$

Again using Eq. (2.57), we get:

$$v_2 = nL_m \frac{di_1}{dt} + n^2 L_m \frac{di_2}{dt} \tag{2.64}$$

Rewriting Eqs. (2.60) and (2.64), we get the following matrix form:

$$\begin{pmatrix} v_1 \\ v_2 \end{pmatrix} = \begin{pmatrix} L_a + L_m & nL_m \\ nL_m & n^2 L_m \end{pmatrix} \begin{pmatrix} \dot{i}_1 \\ \dot{i}_2 \end{pmatrix} \tag{2.65}$$

The equations above do indeed model a pair of linear time-invariant coupled inductors.

The physical interpretations of L_a and L_m are as follows: L_a is the **leakage inductance**, that is, the inductance seen at the first port due to the leakage flux, i.e., the lines of magnetic field that do not link both coils. Indeed, from Exercise 2.2, as $n^2 \to 1$, $M^2 \to L_{11}L_{22}$ and thus $L_a \to 0$. L_m is called the **magnetizing inductance**: its role is to model the magnetic flux common to both coils.

Suppose we wish to build a high-quality transformer. We choose a torus of magnetic material with a very high permeability μ (e.g., ferrite, etc.). We then wind tightly on the torus the two coils forming a two-part, as in Fig. 2.20. Suppose that we are able to find magnetic materials with increasingly high μ: As μ becomes larger and larger, the leakage flux would get smaller and hence $L_a \to 0$. Also, the common flux would keep increasing, hence $L_m \to \infty$. Referring to Fig. 2.22, we see that we are left with an ideal-transformer!

2.2.4 *Three-Terminal Capacitors*

Analogous to a three-terminal inductor, we will define a three-terminal capacitor using the form:

$$q_1 = q_1(v_1, v_2) \tag{2.66}$$

$$q_2 = q_2(v_1, v_2) \tag{2.67}$$

Considering q_1 and q_2 to be linear functions of v_1, v_2 and using the fact that a capacitor is a dual of the inductor, we get:

$$i_1(t) = C_{11}\frac{dv_1}{dt} + C_{12}\frac{dv_2}{dt} \tag{2.68}$$

$$i_2(t) = C_{21}\frac{dv_1}{dt} + C_{22}\frac{dv_2}{dt} \tag{2.69}$$

Physical three-terminal capacitors are beyond the scope of this book. Nevertheless, nonlinear three-terminal capacitors find a variety of applications such as parametric amplification in solid-state circuits [9].

2.3 Three-Terminal Memristors

Finally, we have the three-terminal memristor:

$$\phi_1 = \phi_1(q_1, q_2) \tag{2.70}$$

$$\phi_2 = \phi_2(q_1, q_2) \tag{2.71}$$

We will not discuss three-terminal memristors as they are no physical examples yet. However, the possibility of their future availability cannot be dismissed.

2.4 The Three-Port Circulator

Circulators[3] are very useful microwave devices, used in communication systems and measurements. An **ideal three-port circulator** is a linear circuit element specified

[3]This section was added after a discussion on June 6th 2017, with Dr. Yuping Huang from the Stevens Institute of Technology. His group uses circulators in optical quantum computing applications.

by the following three equations:

$$f_1(v_1, v_2, v_3, i_1, i_2, i_3) \triangleq v_1 - Ri_2 + Ri_3 = 0 \tag{2.72}$$

$$f_2(v_1, v_2, v_3, i_1, i_2, i_3) \triangleq v_2 + Ri_1 - Ri_3 = 0 \tag{2.73}$$

$$f_3(v_1, v_2, v_3, i_1, i_2, i_3) \triangleq v_3 - Ri_1 + Ri_2 = 0 \tag{2.74}$$

where R is a real constant called the **reference resistance**. We can recast the equations above in an elegant matrix form:

$$\begin{pmatrix} v_1 \\ v_2 \\ v_3 \end{pmatrix} = \begin{pmatrix} 0 & R & -R \\ -R & 0 & R \\ R & -R & 0 \end{pmatrix} \begin{pmatrix} i_1 \\ i_2 \\ i_3 \end{pmatrix} \tag{2.75}$$

The circuit symbol for a circulator is shown in Fig. 2.23a. Observe that a three-port circulator is **non-energic** because the instantaneous power **entering** the three-port is identically zero, from Fig. 2.23a:

$$\begin{aligned} p_{\text{circulator}} &= v_1 i_1 + v_2 i_2 + v_3 i_3 \\ &= (Ri_2 - Ri_3)i_1 + (-Ri_1 + Ri_3)i_2 + (Ri_1 - Ri_2)i_3 \\ &= 0 \end{aligned} \tag{2.76}$$

Hence, energy is neither stored nor dissipated in the circulator. To demonstrate how energy is being **redistributed**, suppose we connect three identical resistors whose values are chosen equal to R in the setup shown in Fig. 2.23b. Since $v_2 = -Ri_2$ and $v_3 = -Ri_3$, it follows from Eq. (2.75) that

$$\begin{aligned} v_1 &= Ri_2 - Ri_3 \\ -Ri_2 &= -Ri_1 + Ri_3 \\ -Ri_3 &= Ri_1 - Ri_2 \end{aligned} \tag{2.77}$$

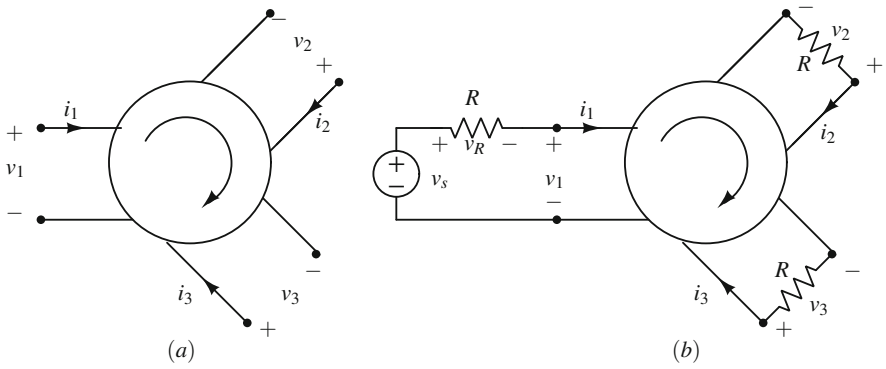

Fig. 2.23 A three-port circulator and a typical application

Solving these equations, we obtain:

$$\begin{aligned} v_1 &= Ri_1 \\ i_1 &= i_2 \\ i_3 &= 0 \end{aligned} \tag{2.78}$$

Now, conservation of energy[4] in the circuit in Fig. 2.23b implies:

$$v_s(-i_1) + v_R i_1 + p_{\text{circulator}} + v_2(-i_2) + v_3(-i_3) = 0 \tag{2.79}$$

But, we have shown that $p_{\text{circulator}} = 0$ and $i_3 = 0$. If we let $p_s = v_s i_1$ be the power supplied by the voltage source, we get:

$$\begin{aligned} p_s &= v_R i_1 + v_2(-i_2) \\ &= Ri_1^2 + Ri_2^2 \\ &= 2(Ri_1^2) \end{aligned} \tag{2.80}$$

We conclude that half of the power supplied by the voltage source is dissipated in its associated series resistor, while the other half is dissipated in the resistor across port 2. In other words, all power entering port 1 is **redirected** to port 2 (to be dissipated in the terminating resistor), with nothing left for port 3 (recall we obtained $i_3 = 0$).

If we repeat the preceding analysis but with the voltage source inserted in port 2, instead of port 1, we will find that all power entering port 2 gets delivered to port 3 with nothing left for port 1. Similarly, inserting the voltage source in port 3, we find that all the power entering port 3 gets delivered to port 1 with nothing left for port 2. Hence, the circulator functions by "circulating" the energy entering one port into the next port **whenever all ports are terminated by resistors equal to the reference resistor** R.

This property is widely exploited in many communication systems for diverting power into various desired channels. For example, the setup in Fig. 2.23b can be used to model the following situation: Let the voltage-source resistor combination model a portable radio transmitter. Let the resistor R across port 2 model an antenna, and let the resistor R across port 3 model a receiver. Because of the circulator, no outgoing signal transmitted from port 1 will reach the receiver. Conversely, any incoming signal from elsewhere that is received by the antenna (when port 1 is not transmitting) will be delivered to the receiver in port 3. Without the circulator, two separate antennas will be needed, one to keep the receiver from receiving its own transmitted signal and the other to keep the transmitter from receiving unwanted signals intended for the receiver.

[4] We could also apply Tellegen's theorem.

2.5 Operational Amplifier (Opamp)

The opamp is an extremely versatile and inexpensive semiconductor device. It has been the workhorse of the electronics hobbyist and students for nearly six decades and hence is of paramount importance.

For **low-frequency** applications, the opamp behaves like a **multi-terminal nonlinear resistor**, which can often be represented by an ideal opamp model. This model greatly simplifies the analysis and design of opamp circuits. In fact, one of the reasons why opamps are so popular is that, at low frequencies,[5] they behave almost like the ideal model! Exercise 2.5 helps the reader understand this justification: the exercise instructs the reader to analyze a typical opamp circuit using the more complicated **finite gain** model and then compare results with those predicted by the ideal opamp model.

Depending on the **dynamic range** of the input signals, the opamp may operate in the **linear** or **nonlinear** region. Section 2.5.2 is devoted to those circuits where the opamp is operating only in the linear region. This restriction allows us to simplify the (nonlinear) ideal opamp model into a **linear** model, called the **virtual short-circuit model**. This model is used extensively in Sect. 2.5.2 for analyzing both simple circuits by **inspection** as well as complicated circuits via a **systematic** method.

In Sect. 2.5.3, we use the nonlinear ideal opamp model to analyze opamps operating in the nonlinear region. We will primarily discuss voltage feedback opamps, but Sect. 2.5.5 will discuss current feedback opamps.

Note that we use a variety of examples. We encourage the reader to simulate these examples using QUCS[6] and also have access to the necessary electronics equipment ("breadboard," etc.) so they can construct the discussed circuits and see opamps "in action."

2.5.1 Device Description, Characteristics, and Model

Opamps are multi-terminal devices, shown in Fig. 2.24, and are sold in several standard packages. For the "breadboard," the most convenient is the DIP (Dual Inline Package) versions of the integrated circuit (IC). Figure 2.25 gives the schematic of the μA741, an opamp introduced by Fairchild Semiconductor in 1968, and still in use today. The seven terminals brought out through the package leads (Fig. 2.24) are labeled **inverting input** IN−, **noninverting input** IN+, **output**

[5] Unless otherwise stated, we will assume that all opamp circuits operate at low enough frequencies so the ideal opamp model is valid.

[6] Although we cover circuit simulation in QUCS in Chap. 3 lab, the reader should be able to use their "native intelligence" to easily simulate the circuits in this chapter, using the QUCS online workbook as a guide.

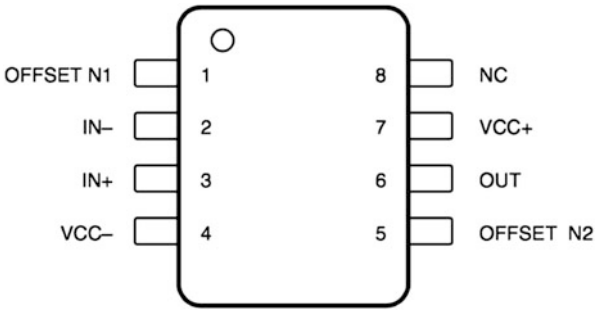

Fig. 2.24 μA741 opamp, in 8-pin SOIC, DIP, and SO versions. Opamp is not to scale

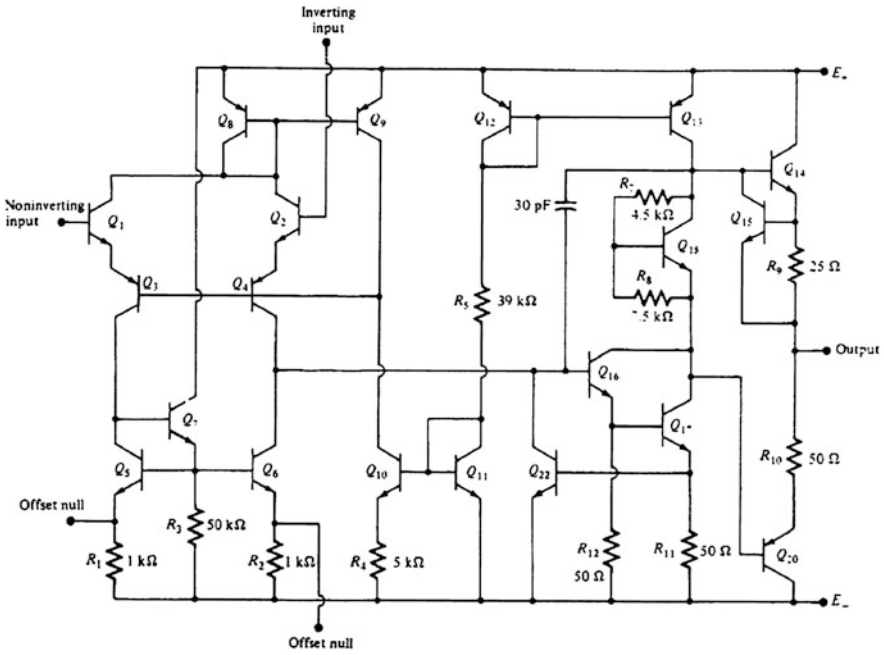

Fig. 2.25 Schematic of the μA741

OUT, **positive power supply** (VCC+), **negative power supply** (VCC−), and **offset nulls** (OFFSET N1, OFFSET N2). The remaining terminals of the package are not connected to the IC and are labeled NC (no connection). The additional terminals such as OFFSET N1 are usually connected to some external nulling or compensation circuit for improving the performance of the opamp. We will not use such external circuits in this book.

Some opamps have more than seven terminals; others have less. For most applications, however, only the five terminals indicated in the standard opamp symbol in Fig. 2.26a are essential. Note that the opamp can be considered a 4-

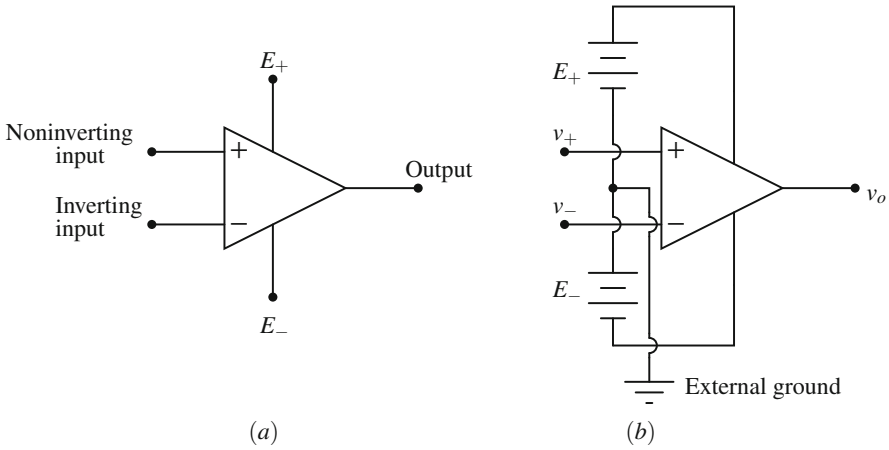

Fig. 2.26 Standard opamp symbol and a typical biasing scheme. (**a**) The + and − signs inside the triangle denote the noninverting and inverting input terminals, respectively. (**b**) A "biased" opamp

terminal device for circuit analysis and design purposes, in the sense that both E_+ and E_- (Fig. 2.26) are referenced to a common external ground. All voltages are also measured with respect to this ground. So, from a circuit theoretic standpoint, we only need v_+, v_-, v_o, and the external ground (four terminals). However, to be consistent with most electronics literature, we will not show the opamp as a four-terminal device. Rather, we will **implicitly assume** that the opamp is connected properly, as in Fig. 2.26b.

In order for the opamp to function properly, its internal transistors must be biased at appropriate operating points (we will discuss small-signal analysis in Sect. 3.1.1, the concept of biasing should become clear then). The power supply terminals are provided for this purpose. In Fig. 2.24, the supplies are labeled as VCC+ and VCC−. The justification for using the CC label is that the μA741 is a BJT opamp, CC is an acronym for "collector." Since other transistor (for example, FET)-based opamps exist, we will use E_+ and E_- for generality.

In general, E_+ and E_- are connected to a split power supply as shown in Fig. 2.26b, with respect to an **external ground**. Typically, $E_+ = 15$ V and $E_- = 15$ V (they do not have to be symmetrical with respect to ground). For clarity purposes, we will henceforth use the symbol shown in Fig. 2.27 (assuming that we have a symmetrical external power supply, $E = \pm 15$ V). In Fig. 2.27a, i_- and i_+ denote the current entering the opamp inverting and noninverting terminals, respectively. Similarly, v_-, v_+, and v_o denote, respectively, the voltage from the inverting terminal, noninverting terminal, and output terminal to ground. The variable v_d in Fig. 2.27b is called the **differential input voltage** and will play an important role in opamp circuit analysis.

To derive an exact characterization of an opamp would require analyzing the entire integrated circuit, such as the one shown in Fig. 2.25. Fortunately, for many

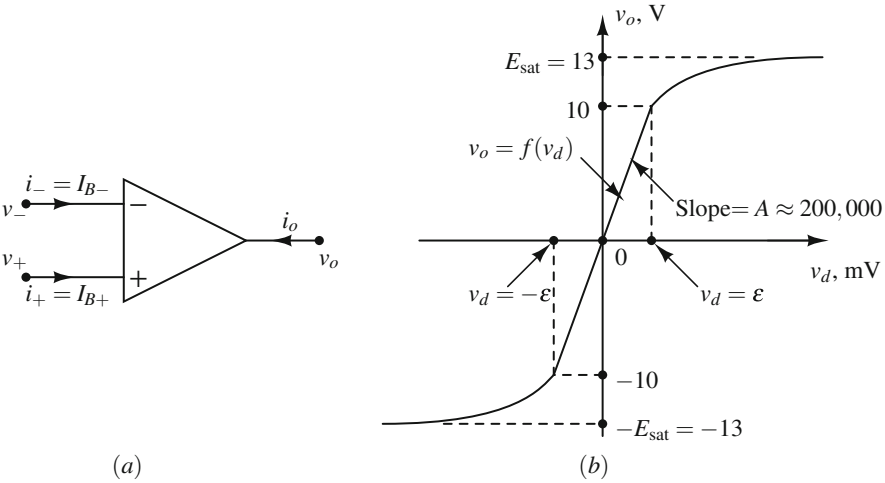

Fig. 2.27 Experimental characterization of a typical opamp. In (**b**), $v_d \triangleq v_+ - v_-$

low-frequency applications, the opamp terminal currents and voltages have been found **experimentally** to obey the following **approximate** relationships:

$$i_- = I_{B-} \tag{2.81}$$

$$i_+ = I_{B+} \tag{2.82}$$

$$v_o = f(v_d) \tag{2.83}$$

where I_{B-} and I_{B+} are called the **input bias currents** and $f(v_d)$ denotes the v_o-vs-v_d **voltage transfer characteristic (VTC)**, since the plot shows how one voltage v_{in} is "transferred" to another voltage v_o.[7] Apart from a scaling factor which depends on the power supply voltage, $f(v_d)$ follows approximately an odd-symmetric function as shown in Fig. 2.27b (drawn for a ± 15 V supply voltage). Moreover, this function has been found to be rather insensitive to changes in the output current i_o.

The transfer characteristic in Fig. 2.27b displays three remarkable properties:

1. v_o and v_d have different scales: one is in volts, the other in millivolts.
2. In a small interval $-\epsilon < v_d < \epsilon$ of the origin, $f(v_d) \approx A v_d$ is nearly **linear** with a very steep slope A—called the **open-loop voltage gain**. It is called "open loop" because there is no feedback in the circuit (that is, the output is not connected back to any of the inputs). This is a terminology from control systems. If there is feedback, we say the loop is "closed" (or "closed loop").

[7] The word "transfer" means that the response variable does not appear at the same port as the source serving as input. There are four types of TCs possible: v_o-vs-v_{in}, v_o-vs-i_{in}, i_o-vs-v_{in}, and i_o-vs-i_{in}.

3. $f(v_d)$ **saturates** at $v_o = \pm E_{\text{sat}}$, where E_{sat} is typically 2 V less than the power supply voltage, if the opamp in question is realized using BJTs. In that case, we say the opamp is not "rail-to-rail." On the other hand, FET opamps usually have rail-to-rail behavior and E_{sat} for such FET opamps usually range from E_- to E_+.

Also, the bias currents for opamps using BJTs as inputs are much larger than opamps that use FET input transistors. For example, the **average** input bias current $I_B \triangleq \frac{1}{2}(|I_{B+}| + I_{B-}|)$ is equal to 0.1 mA for the μA741 but only 0.1 nA for the μA740 (which uses a part of FET input transistors).

The open-loop voltage gain A is typically equal to at least 100,000 (200,000 for the μA741). On the other hand, the voltage ϵ at the end of the **linear** region in Fig. 2.27b is typically less than 0.1 mV.

In view of the typical magnitudes of $I_{\text{B}-}$, $I_{\text{B}+}$, A, and ϵ, little accuracy is lost by assuming $I_{\text{B}-} = I_{\text{B}+} = \epsilon = 0$, $A \to \infty$. This simplifying assumption leads to the **ideal** opamp model shown in Fig. 2.28. To emphasize that $A \to \infty$ in the linear region, we added ∞ inside the triangle to distinguish the **ideal** opamp symbol from other models. Unless otherwise stated, the ideal opamp model will be used throughout this book. Note that the VTC of the ideal opamp model reduces to the three-segment PWL characteristic shown in Fig. 2.28a. The ideal opamp model can be described analytically as follows:

$$i_- = 0 \tag{2.84}$$

$$i_+ = 0 \tag{2.85}$$

$$v_o = E_{\text{sat}} \frac{|v_d|}{v_d}, \quad v_d \neq 0 \tag{2.86}$$

$$v_d = 0, \quad -E_{\text{sat}} < v_o < E_{\text{sat}} \tag{2.87}$$

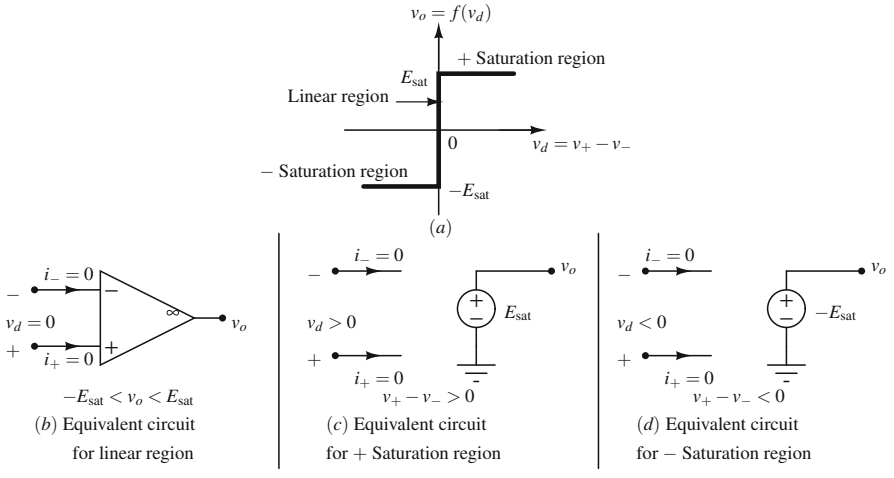

Fig. 2.28 Ideal opamp model

Because these equations are rather cumbersome and difficult to manipulate analytically, it is more practical to represent each region by the simple equivalent circuits shown in Fig. 2.28b, c, and d. Note that these three equivalent circuits contain exactly the same information as Eq. (2.84) through (2.87). In particular, when the opamp is operating in the linear region, the ideal opamp model reduces to that shown in Fig. 2.28b. Note that in the linear region, v_d is constrained to be zero at all times while $|v_o|$ is constrained to be less than the saturation voltage E_{sat}. Hence, the circuit is described by Eqs. (2.84), (2.85), and (2.87).

The circuit in Fig. 2.28c is described by Eqs. (2.84), (2.85), and (2.86) with $v_d > 0$. Likewise, the circuit in Fig. 2.28d is described by Eqs. (2.84), (2.85), and (2.86) with $v_d < 0$.

Opamp circuits designed to operate exclusively in the linear region are analyzed in Sect. 2.5.2. Note that although the opamp is operating in the linear region, the circuit itself may contain nonlinear elements. Opamp circuits operating in both linear and nonlinear regions will be analyzed in Sect. 2.5.3.

Example 2.5.1 The datasheet for a μA741 shows a typical open-loop voltage gain of 200,000. Calculate the value of ϵ for a power supply voltage of ± 20 V. Assume E_{sat} = magnitude of power supply voltage ± 2 V (use $\pm$ as appropriate).

Solution Given the information above, we have $E_{\text{sat}} = \pm 18$ V. Hence:

$$\begin{aligned} \epsilon &= \frac{\pm 18 \text{ V}}{200000} \\ &= \pm 0.09 \text{ mV} \end{aligned} \tag{2.88}$$

Example 2.5.2 An opamp manufacturer's datasheet usually specifies the typical value of the average input bias current I_B (defined earlier as $\frac{1}{2}(|I_{B+}| + |I_{B-}|)$) and the offset current $I_{\text{os}} \triangleq |I_{B+}| - |I_{B-}|$. Express $|I_{B+}|$ and $|I_{B-}|$ in terms of I_B and I_{os}.

Solution From the definition of I_B, we get:

$$2I_B = |I_{B+}| + |I_{B-}| \tag{2.89}$$

Adding the equation above to the definition of I_{os}, we get:

$$2I_B + I_{\text{os}} = 2|I_{B+}| \tag{2.90}$$

(continued)

Example 2.5.2 (continued)
Subtracting the definition of I_{os} from the equation for $2I_B$, we get:

$$2I_B - I_{os} = 2|I_{B-}| \tag{2.91}$$

Hence, we have:

$$|I_{B+}| = \frac{1}{2}(2I_B + I_{os}) \tag{2.92}$$

$$|I_{B-}| = \frac{1}{2}(2I_B - I_{os}) \tag{2.93}$$

2.5.2 *Linear Opamp Circuits*

The methods to be developed in this section are valid **only** if the opamp output voltage satisfies

$$-E_{sat} < v_o(t) < E_{sat} \tag{2.94}$$

for all times t. We will henceforth refer to the expression in Eq. (2.94) as the **validating inequality** for the **linear** region. If this inequality is violated in any time interval $[t_1, t_2]$, the solution in this interval is incorrect and must be recalculated using the nonlinear model from Sect. 2.5.3.

Recall from Fig. 2.1 in Sect. 2.1 that a three-port is characterized by three relationships among the associated voltage and current variables. Notice that in the linear region, the ideal opamp in Fig. 2.28b can be described analytically by the three equations[8]:

$$i_- = 0 \tag{2.95}$$

$$i_+ = 0 \tag{2.96}$$

$$v_+ - v_- = 0 \tag{2.97}$$

[8]These correspond to Eqs. (2.84), (2.85), and (2.87).

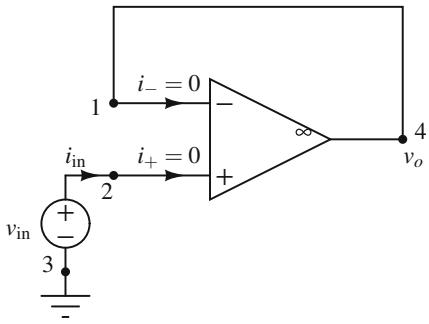

Fig. 2.29 The voltage follower, or unity-gain buffer

Consequently, we can think of the ideal opamp model in Fig. 2.28b as a three-port.[9] For purposes of analysis, Eqs. (2.95) through (2.97) are equivalent to:

1. Connecting a **short circuit** across the opamp input terminals.
2. Stipulating that the **currents** through the **input terminals are zero at all times**.

To emphasize the special nature of this short circuit, we will henceforth refer to the model from Eqs. (2.95) through (2.97) as the **virtual short-circuit model**. Notice that the word "virtual" is very important, $v_+ = v_-$ because of the opamp, not because v_+ is physically connected to v_-.

Using the virtual short-circuit model, many opamp circuits can be analyzed by inspection. This method usually requires no more than three calculations and is often implemented by invoking KCL and Eqs. (2.95) through (2.97) mentally, perhaps with an occasional scribble on the "back of an envelope." It is best illustrated via some useful opamp circuits as examples.

Example 2.5.3 Determine the v_o-vs-v_{in} VTC for the circuit in Fig. 2.29.

Solution First, let us apply KCL at node 2 and obtain:

$$i_{\text{in}} = i_+ = 0 \tag{2.98}$$

Applying next KVL around the closed node sequence $4 - 3 - 2 - 1 - 4$:

$$-v_o + v_{\text{in}} - v_d = 0 \tag{2.99}$$

(continued)

[9] Recall that an opamp always has an external reference terminal, hence an ideal opamp can also be considered as a four-terminal resistor.

Example 2.5.3 (continued)
where we have used the usual definition: $v_d = v_+ - v_-$. But, because of the virtual short-circuit model $v_d = 0$, so:

$$v_o = v_{\text{in}} \tag{2.100}$$

To complete the analysis, we apply the validating inequality from Eq. (2.94) and obtain:

$$-E_{\text{sat}} < v_{\text{in}} < E_{\text{sat}} \tag{2.101}$$

This gives the dynamic range of input voltages beyond which the opamp no longer operates in the linear region.

Note that the voltage follower in Example 2.5.3 defines a unity-gain VCVS. This circuit has an infinite input resistance because $i_{\text{in}} = 0$ and its output "duplicates" the input voltage, regardless of the external load. Consequently, it is also called an **isolation amplifier**. It is widely used between 2 two-ports to prevent one two-port from "loading down" the other two-port. This isolation technique is one of the most useful tools in a designer's "toolbox."

Example 2.5.4 Determine the v_o-vs-v_{in} VTC for the inverting amplifier circuit in Fig. 2.30. Note that this circuit contains linear resistors, as opposed to the voltage follower.

Solution Since $v_d \triangleq v_+ - v_- = 0$, we have:

$$v_1 = v_{\text{in}} \tag{2.102}$$

By Ohm's law:

$$i_1 = \frac{v_1}{R_1} \tag{2.103}$$

Since $i_- = 0$, we have $i_2 = i_1$. Hence:

$$v_2 = R_f i_1 = R_f \left(\frac{v_{\text{in}}}{R_1} \right) \tag{2.104}$$

(continued)

Example 2.5.4 (continued)
Applying KVL around the closed node sequence $4-2-1-4$:

$$v_o = \left(\frac{-R_f}{R_1}\right) v_{\text{in}} \tag{2.105}$$

To complete the analysis, we apply the validating inequality from Eq. (2.94) and obtain:

$$\left(-\frac{R_1}{R_f}\right) E_{\text{sat}} < v_{\text{in}} < \left(\frac{R_1}{R_f}\right) E_{\text{sat}} \tag{2.106}$$

Hence, so long as the input signal satisfies Eq. (2.106), the circuit functions as a voltage amplifier with voltage gain equal to $-R_f/R_1$ (assuming $R_f > R_1$).

Exercise 2.3 gives an example of a noninverting amplifier configuration. Of course, we can have nonlinear elements in conjunction with the ideal opamp model, exercise 2.4 shows one such circuit that functions as a "clipper." Note again the versatility of the ideal opamp model comes from the fact that even if we did assume that the open-loop gain A is finite, the answers obtained using a **finite gain model** are nearly identical to the results from the ideal opamp model. Exercise 2.5 explores this further.

The inspection method often fails whenever it is necessary to solve two or more simultaneous equations. In such cases, it is desirable to develop a systematic method for writing a system of linearly independent equations involving as few variables as possible. The following example illustrates the basic steps involved.

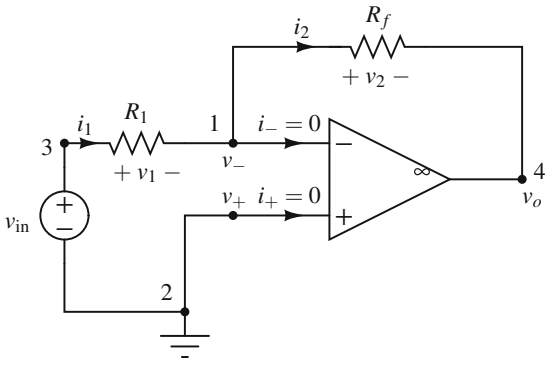

Fig. 2.30 The inverting amplifier

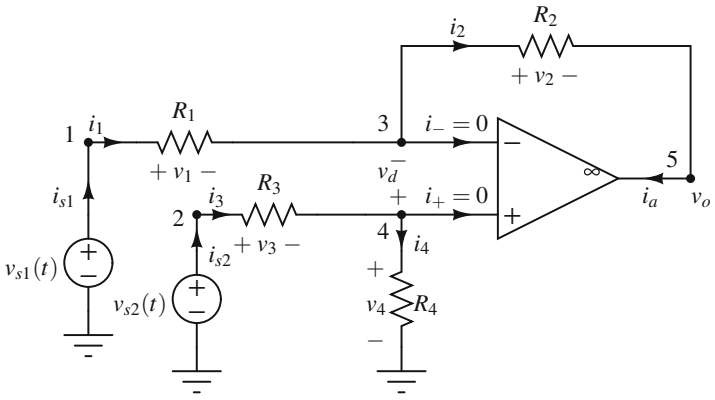

Fig. 2.31 An opamp summing amplifier for illustrating the systematic method

Example 2.5.5 Consider the opamp circuit in Fig. 2.31. Determine the VTC for this circuit using the systematic method.

Solution Although this circuit can be solved by inspection, we will leave that to the reader as an exercise. Given below are the steps for the systematic method approach:

1. Label the nodes consecutively and let e_j denote as usual the voltage from node j to the ground node. In our case, $j = 1, 2, \cdots, 5$. Express **all** resistor voltages and the differential opamp voltage v_d in terms of the node-to-ground voltages via KVL:

$$v_1 = e_1 - e_3 \tag{2.107}$$

$$v_2 = e_3 - e_5 \tag{2.108}$$

$$v_3 = e_2 - e_4 \tag{2.109}$$

$$v_4 = e_4 \tag{2.110}$$

$$v_d = e_4 - e_3 \tag{2.111}$$

2. Express the branch current in each linear resistor in terms of node-to-ground voltages via Ohm's law:

$$i_1 = \frac{e_1 - e_3}{R_1} \tag{2.112}$$

$$i_2 = \frac{e_3 - e_5}{R_2} \tag{2.113}$$

(continued)

Example 2.5.5 (continued)

$$i_3 = \frac{e_2 - e_4}{R_3} \tag{2.114}$$

$$i_4 = \frac{e_4}{R_4} \tag{2.115}$$

3. Identify all other branch **current** variables which **cannot** be expressed in terms of node-to-ground voltages, namely, the currents i_{s1}, i_{s2}, and i_a. Note that the opamp input currents i_- and i_+ are not variables in an ideal opamp model, because they are equal to zero. Our objective is to write a system of linearly independent equations in terms of node-to-ground voltages and the **identified** current variables $\{i_{s1}, i_{s2}, i_a\}$.
4. Write KCL at each node (except the ground node) in terms of $\{e_1, e_2, e_3, e_4, e_5, i_{s1}, i_{s2}, i_a\}$:

$$\text{Node 1:} \quad \frac{e_1 - e_3}{R_1} = i_{s1} \tag{2.116}$$

$$\text{Node 2:} \quad \frac{e_2 - e_4}{R_3} = i_{s2} \tag{2.117}$$

$$\text{Node 3:} \quad \frac{e_3 - e_5}{R_2} = \frac{e_1 - e_3}{R_1} \tag{2.118}$$

$$\text{Node 4:} \quad \frac{e_4}{R_4} = \frac{e_2 - e_4}{R_3} \tag{2.119}$$

$$\text{Node 5:} \quad i_a = \frac{e_3 - e_5}{R_2} \tag{2.120}$$

5. Eqs. (2.116) through (2.120) consists of five equations with eight variables. Hence, we need to write three more independent equations. Since we have already made use of KVL (Step 1), KCL (Step 4), and the resistor characteristics (Step 2), these three equations must come from the characteristics of the voltage sources and the opamp:

$$e_1 = v_{s1} \tag{2.121}$$

$$e_2 = v_{s2} \tag{2.122}$$

$$e_4 - e_3 = 0 \tag{2.123}$$

(continued)

Example 2.5.5 (continued)

6. Together, the equations in the previous two steps constitute a system of eight linearly independent equations in terms of eight variables. Solving these equations for the desired opamp output voltage $v_o = e_5$ by any elimination or any other method, we obtain:

$$v_o = \left[\frac{R_4(1 + R_2/R_1)}{R_3 + R_4}\right] v_{s2}(t) - \left(\frac{R_2}{R_1}\right) v_{s1}(t) \tag{2.124}$$

7. Determine the dynamic range of the input voltages for which Eq. (2.124) holds, i.e., where the opamp is operating in the linear region:

$$-E_{\text{sat}} < \left[\frac{R_4(1 + R_2/R_1)}{R_3 + R_4}\right] v_{s2}(t) - \left(\frac{R_2}{R_1}\right) v_{s1}(t) < E_{\text{sat}} \tag{2.125}$$

We should of course perform some sanity checks for Example 2.5.5. For example, if $v_{s2} = 0$, we obtain an inverting amplifier. The expression and dynamic range correctly reduce to the corresponding expressions for an inverting amplifier.

We could have also quite easily derived Eqs. (2.124) and (2.125) by using the inspection method: since R_3 and R_4 are in series, we can quickly obtain an expression for e_4 and simply write a KCL expression at e_3 (since $e_3 = e_4$ by the virtual short-circuit model). The point of the example was to illustrate the systematic method.

The preceding systematic method is applicable to any opamp circuit containing linear resistors, independent voltage, and current sources, and opamps modeled by virtual short circuits. This method will be generalized in Sect. 4.2.2.1, called **modified nodal analysis (MNA)**, for arbitrary circuits.

2.5.2.1 Implementation of Dependent Sources

A very elegant opamp application is implementation of dependent sources. In fact, the inverting amplifier from Exercise 2.3 is an example of a VCVS. We will consider the implementation of the other dependent sources in the examples below.

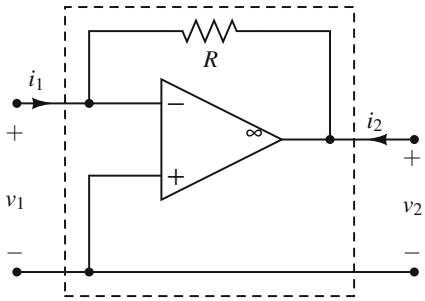

Fig. 2.32 CCVS using opamp

Example 2.5.6 The circuit in Fig. 2.32 (boxed to highlight the two-port variables) implements a linear CCVS. Determine the transresistance r_m and the dynamic range for the opamp.

Solution We can easily derive the two-port CCVS relationship in Eq. (2.24) using the inspection method. Since $v_1 = v_- - v_+$, we have:

$$v_1 = 0 \tag{2.126}$$

Applying Ohm's law:

$$v_1 - v_2 = i_1 R \tag{2.127}$$

Thus:

$$v_2 = -Ri_1 \tag{2.128}$$

Hence, the transresistance $r_m = -R$. Applying the validating inequality and using the relationship between v_2 and i_1 derived above, we get the dynamic range:

$$-\frac{E_{\text{sat}}}{R} < i_1 < \frac{E_{\text{sat}}}{R} \tag{2.129}$$

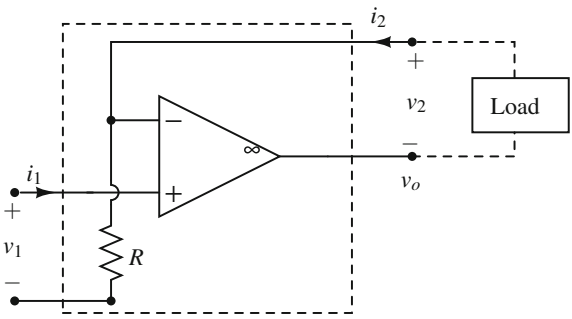

Fig. 2.33 VCCS using opamp

Example 2.5.7 The circuit in Fig. 2.33 (boxed to highlight the two-port variables) implements a linear VCCS. Determine the transconductance g_m and the dynamic range for the opamp.

Solution We can easily derive the two-port VCCS relationship in Eq. (2.25) using the inspection method. Since $i_1 = i_+ = 0$, we have:

$$i_1 = 0 \tag{2.130}$$

Applying Ohm's law and using the virtual short-circuit model, we get:

$$i_2 = \frac{v_1}{R} \tag{2.131}$$

Hence, the transconductance $g_m = \frac{1}{R}$. From KVL: $v_1 - v_2 = v_o$ and applying the validating inequality, we get the dynamic range:

$$v_2 - E_{\text{sat}} < v_1 < v_2 + E_{\text{sat}} \tag{2.132}$$

Example 2.5.8 The circuit in Fig. 2.34 (boxed to highlight the two-port variables) implements a linear CCCS. Determine the current gain α and the dynamic range for the opamp.

Solution This circuit illustrates the importance of understanding that an opamp is biased via external power supplies. Our goal is to derive Eq. (2.26) using the inspection method. Applying KVL around loop $1 - 2 - 3 - 4 - 1$

(continued)

Example 2.5.8 (continued)
and using node-to-ground voltages, we get:

$$(e_1 - e_2) + (e_2 - e_3) + (e_3 - e_4) = 0 \tag{2.133}$$

We will simplify the KVL equation by first noting that the opamp virtual short-circuit model implies $e_1 = e_4$. We will then apply Ohm's law to resistors R_1, R_2 and use KCL at node 2. Thus, we can simplify the KVL equation to:

$$i_1 R_1 + (i_1 - i_2) R_2 = 0 \tag{2.134}$$

We thus have:

$$i_2 = \left(1 + \frac{R_1}{R_2}\right) i_1 \tag{2.135}$$

Therefore, the current gain for the CCCS is $\alpha = 1 + \frac{R_1}{R_2}$. Since $e_1 = e_4 = 0$, we get from KVL:

$$-i_1 R_1 + v_2 = v_o \tag{2.136}$$

Now, we can apply the validating inequality:

$$-E_{\text{sat}} < -i_1 R_1 + v_2 < E_{\text{sat}} \tag{2.137}$$

Simplifying:

$$E_{\text{sat}} > i_1 R_1 - v_2 > -E_{\text{sat}} \tag{2.138}$$

Hence, the dynamic range is:

$$\frac{v_2 - E_{\text{sat}}}{R_1} < i_1 < \frac{v_2 + E_{\text{sat}}}{R_1} \tag{2.139}$$

2.5.3 *Nonlinear Opamp Circuits*

There are many applications where the opamp operates in all three regions of the ideal opamp model in Fig. 2.28. This occurs whenever the amplitudes of one or more input signals are such that the validating inequality in each region is violated over some time intervals. In this case, we probably have to use **all** three regions in Fig. 2.28 and we say that the opamp is "nonlinear." Fortunately, since the

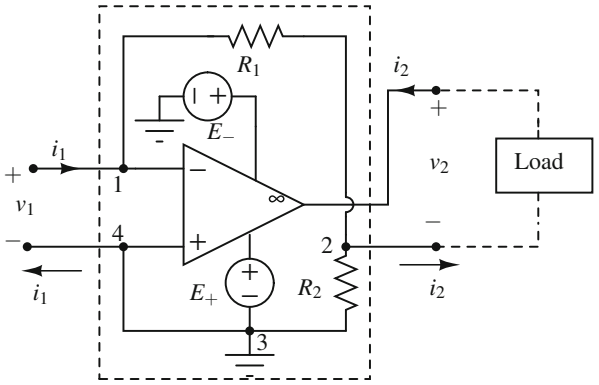

Fig. 2.34 CCCS using opamp

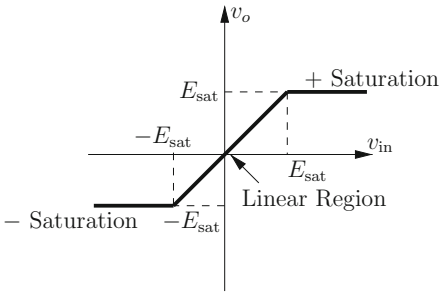

Fig. 2.35 VTC of a voltage follower

characteristic in Fig. 2.28a is a **PWL** characteristic, the circuit in each region can be easily analyzed as a linear circuit.

Most practical nonlinear opamp circuits involve the use of **positive feedback**: the output is connected to the **noninverting** input. The mindful reader would have noticed that all the circuits in the preceding section involved **negative feedback**: the output was connected to the **inverting** input. Inherently, negative feedback is stable while positive feedback is not. However, stability is a **dynamic** concept and understanding specifically opamp positive feedback requires the use of first-order circuits (to be discussed in Sect. 4.2.1). But, the **fact** that positive feedback **is different** from negative feedback can be easily explained using the PWL model, as discussed below.

Recall the voltage follower from Example 2.5.3. We plot the VTC for the follower in Fig. 2.35.

What happens if we interchange the inverting and noninverting terminals as shown in Fig. 2.36? By inspection, we can find $v_o = v_{\text{in}}$ provided $|v_{\text{in}}| < E_{\text{sat}}$. Hence, in the linear region, the transfer characteristic of this positive feedback circuit is identical to that of the voltage follower VTC in Fig. 2.35. In practice, however, they do not behave in the same way: One functions as a voltage follower, the other **does not**. To uncover the reason, let us derive the transfer characteristics in the remaining regions.

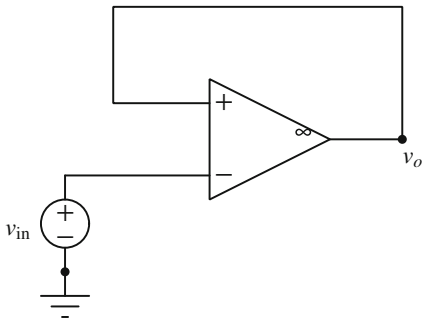

Fig. 2.36 A positive feedback circuit

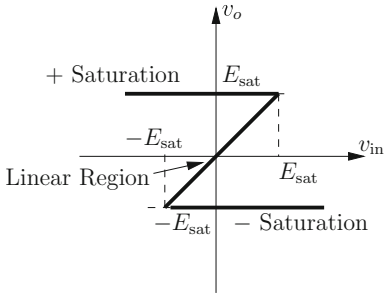

Fig. 2.37 VTC of the positive feedback circuit from Fig. 2.36

When the opamp is in the + Saturation region, the validating inequality from Fig. 2.28b for the circuit in Fig. 2.36 becomes: $v_d = E_{\text{sat}} - v_{\text{in}} > 0$ or $v_{\text{in}} < E_{\text{sat}}$. Hence, the transfer characteristic in this region is given by $v_o = E_{\text{sat}}$ whenever $v_{\text{in}} < E_{\text{sat}}$, as shown in Fig. 2.37.

Conversely, when the opamp is in the − Saturation region, the validating inequality from Fig. 2.28c becomes: $v_d = -E_{\text{sat}} - v_{\text{in}} < 0$ or $v_{\text{in}} > -E_{\text{sat}}$. Hence, the transfer characteristic in this region is given by $v_o = -E_{\text{sat}}$ whenever $v_{\text{in}} > -E_{\text{sat}}$, completing the VTC in Fig. 2.37.

Note that complete transfer characteristics in Figs. 2.35 and 2.37 are quite different. Even if the opamp is operating in the linear region ($|v_{\text{in}}| < E_{\text{sat}}$), there are three distinct output voltages for each value of v_{in} for the positive feedback circuit. Using a more realistic opamp circuit model to be developed in Chap. 4, we will show that all operating points on the middle segment (linear region) in Fig. 2.37 are **unstable**. The important concepts of **stability** and **instability** will be discussed in Chap. 4. In the present context, having **unstable operating points** in the middle region means that even if the voltage $v_{\text{in}}(0)$ lies on this segment, it will quickly move to the + Saturation region if $v_{\text{in}}(0) > 0$ or into the negative saturation region if $v_{\text{in}}(0) < 0$.

One may wonder if we can even confirm the VTC in Fig. 2.37 experimentally, since the linear region is unstable. The lab component for this chapter shows how to confirm an equivalent VTC for a Schmitt trigger (discussed below), by using an elegant mathematical trick. The Schmitt trigger is actually a very elegant application

of positive feedback that illustrates the very important concept that stability is a dynamic phenomenon.

2.5.3.1 Schmitt Trigger

Consider the circuit shown in Fig. 2.38.

The Schmitt trigger in Fig. 2.38 is used for signal conditioning in the presence of noise: the output is $\pm E_{\text{sat}}$ depending on the input voltage, but the **physical** circuit also displays **hysteresis or memory**. That is, the output voltage depends on the **derivative** of the input voltage. The advantages offered by the Schmitt trigger when compared to the simple positive feedback circuit in Fig. 2.36 are: we can control the slope of the linear region and the values of the "trip" voltages V^+ and V^- (in the Schmitt trigger VTC in Fig. 2.39), using R_1 and R_2.

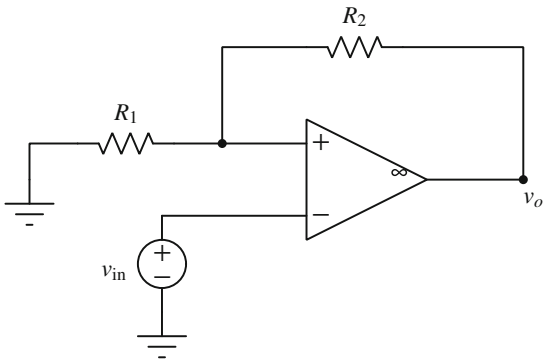

Fig. 2.38 The inverting Schmitt trigger

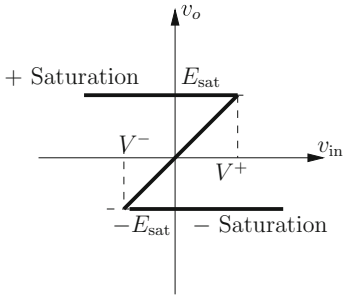

Fig. 2.39 VTC of the inverting Schmitt trigger in Fig. 2.38. Compare to the simple positive feedback VTC in Fig. 2.37

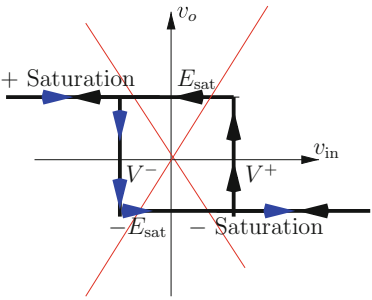

Fig. 2.40 An incorrect VTC for the inverting Schmitt trigger in Fig. 2.38. It is incorrect because the arrows on the VTC specify dynamic behavior, whereas the circuit in Fig. 2.38 does not include any dynamic elements

Note the emphasis on the word physical when discussing hysteresis: the justification for the hysteretic behavior is the presence of parasitic components (such as capacitors) in the physical implementation (to be discussed in Sect. 4.2.1). Most people fail to separate the **static VTC characteristic** implied by Fig. 2.38 and **incorrectly** derive the VTC of the Schmitt trigger, shown in Fig. 2.40.

Unfortunately, the VTC in Fig. 2.40 combines both static and dynamic characteristics, whereas Fig. 2.38 does not have any dynamic elements (capacitors, inductors, and memristors). Hence, we will now derive the correct VTC shown in Fig. 2.39 for the Schmitt trigger in Fig. 2.38, by simply using our ideal opamp model from Fig. 2.28.

Example 2.5.9 Derive the v_o-vs-v_{in} expressions for the inverting Schmitt trigger in Fig. 2.38, and hence justify the VTC in Fig. 2.39.

Solution Assuming the opamp is in the linear region of operation and applying KCL at the noninverting input, we get using the inspection method:

$$\frac{0 - v_{\text{in}}}{R_1} = \frac{v_{\text{in}} - v_o}{R_2} \tag{2.140}$$

Simplifying:

$$v_o = v_{\text{in}} \left(1 + \frac{R_2}{R_1}\right) \tag{2.141}$$

Notice that as $R_1 \to \infty$ (an open circuit), we get $v_o = v_{\text{in}}$ from Eq. (2.141). This obviously agrees with the slope of the linear region being equal to 1 for the simple positive feedback circuit in Fig. 2.36. Also, notice that as long as $R_2 \not\to \infty$ in Fig. 2.38, the value of R_2 is irrelevant if $R_1 \to \infty$, since the current into the noninverting input is zero and hence there is no voltage drop across R_2. Note that both R_1 and R_2 tending to ∞ means that the circuit

(continued)

Example 2.5.9 (continued)
is physically ill-defined: the noninverting input is floating (not connected to anything).

Applying the validating inequality for the + Saturation region, we get:

$$v_+ - v_- > 0 \tag{2.142}$$

Simplifying:

$$v_{\text{in}} < \left(\frac{R_1}{R_1 + R_2}\right) E_{\text{sat}} \tag{2.143}$$

Thus, $V^+ = \left(\frac{R_1}{R_1+R_2}\right) E_{\text{sat}}$. Analogously, we can derive an expression for V^-, applying the validating inequality for the − Saturation region, we get:

$$v_{\text{in}} > -\left(\frac{R_1}{R_1 + R_2}\right) E_{\text{sat}} \tag{2.144}$$

Hence, $V^- = -\left(\frac{R_1}{R_1+R_2}\right) E_{\text{sat}}$.

The example above discussed the inverting Schmitt trigger. Exercise 2.6 explores the noninverting Schmitt trigger.

2.5.3.2 PWL Circuits

Consider the circuit shown in Fig. 2.41a, reproduced from the epigraph to this chapter. Our goal is to derive the DP characteristic. As before, we can use the inspection method.

We note that R_1 and R_2 form a voltage divider so that:

$$\begin{aligned} e_3 &= \frac{R_2}{R_1 + R_2} v_o \\ &= \beta v_o \end{aligned} \tag{2.145}$$

If the opamp is operating in the linear region, $e_3 = v$. Hence, substituting for e_3 in the equation above, we get:

$$v_o = \frac{1}{\beta} v \tag{2.146}$$

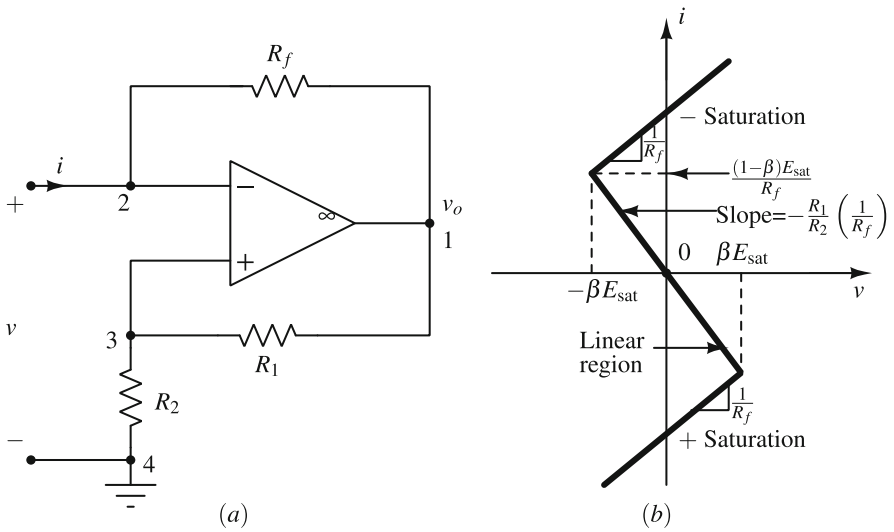

Fig. 2.41 A negative-resistance converter, and its DP characteristic. Here, $\beta \triangleq R_2/(R_1 + R_2)$

Applying KVL around the close node sequence $4 - 1 - 2 - 4$, we get:

$$v = v_o + R_f i \tag{2.147}$$

In Eq. (2.147), we have used that the fact the current into the inverting input of the opamp is zero. Using Eqs. (2.146) and (2.147), we can obtain i-vs-v for the opamp operating in the linear region:

$$i = -\left(\frac{R_1}{R_2}\right)\left(\frac{1}{R_f}\right)v \tag{2.148}$$

Next, we will use the validating inequality to conditions on v for the opamp to be operating in the linear region:

$$-\beta E_{\text{sat}} < v < \beta E_{\text{sat}} \tag{2.149}$$

Notice that obtaining the $i - v$ relationships for the saturation regions is trivial, since Eq. (2.147) is valid for any opamp region of operation, thus:

$$v = \pm E_{\text{sat}} + R_f i \tag{2.150}$$

Specifically, for the + Saturation region:

$$i = \frac{1}{R_f}v - \frac{1}{R_f}E_{\text{sat}} \tag{2.151}$$

For the − Saturation region:

$$i = \frac{1}{R_f} v + \frac{1}{R_f} E_{\text{sat}} \tag{2.152}$$

Equations (2.148), (2.151), and (2.152) complete the DP plot in Fig. 2.41b. The circuit is called a **negative impedance converter (NIC)** because it converts positive resistances R_1, R_2, R_f into a **negative resistance** equal to $-\frac{R_2 R_f}{R_1}$ in the opamp's linear region of operation.

Exercise 2.7 asks the reader to experimentally measure the DP plot for Fig. 2.41a. For more examples of practical negative-resistance opamp circuits, see [5].

We will see in Chapter 4 how this circuit can be used to build a relaxation oscillator. We will also see the enormous advantage of PWL analysis when we cover dynamic nonlinear networks in Chap. 4: PWL techniques allows us to derive closed-form expressions for the period (and frequency), that agree remarkable well with measured values. Moreover, that chapter will show the enormous importance of nonlinear circuit theory in designing a very important class of circuits—oscillators.[10]

2.5.4 A Family of Two-Port Resistors

The functions performed by the opamp circuits discussed so far can be summarized in one statement: They transform input voltage waveforms (functions of time) into some desired output voltage waveforms (functions of time). It is important to observe that the independent variable of the transformation is always time t.

There is another important class of networks which also performs certain transformations, but the independent variable is not time. This class of networks takes the form of a two-port black box, and is in fact a **two-port resistor**. If we connect a nonlinear resistor across port 2 of this two-port resistor, as shown in Fig. 2.42, the resulting two-terminal black box can be interpreted as a new nonlinear resistor because it will have a $v_1 - i_1$ curve different from the original $v - i$ curve. In other words, the function performed by the two-port resistor is that of transforming a given $v - i$ curve into a new $v_1 - i_1$ curve. In this sense, we can generate many new nonlinear resistors from those that are presently available commercially. Of course, an arbitrary transformation is not likely to do us much good. What we need is to discover a few basic transformations from which all others can be obtained. Amazingly, only three types of transformations are necessary, a scaling transformation, a rotation transformation, and a reflection transformation.

[10]The linear oscillator, modeled by an LC network, requires zero resistance for sustained oscillations. Since zero resistance is near impossible to obtain physically (save for superconductors), all practical oscillators are nonlinear.

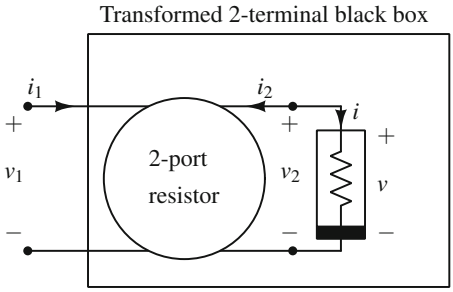

Fig. 2.42 The $v - i$ curve of a given nonlinear resistor is transformed into a new $v_1 - i_1$ curve by connecting the resistor across one port of a two-port resistor

In the scaling transformation, the abscissa or the ordinate of each point on the $v - i$ curve is multiplied by a positive constant k. Such two-port resistors are accordingly called **scalors**.

In the rotation transformation, the original $v - i$ curve is rotated through an angle θ with respect to the origin. Such two-port resistors are accordingly called **rotators**.

In the reflection transformation, the original $v - i$ curve is reflected (the mirror image) with respect to some straight line through the origin. Such two-port resistors are accordingly called **reflectors**.

In the next section, we will mostly give a high-level overview of each of these devices. Implementation details can be found in [3] or in the accompanying online material(s) to this book. However, the reader should notice that these high-level implementations reuse a variety of components (such as controlled sources) from our earlier discussions. Obviously, we realized controlled sources using opamps. Thus, at the implementation level, opamps play a vital role in realizing the family of two-port resistors.

2.5.4.1 Scalors, Rotators, and Reflectors

There are two types of scalors, **voltage scalor** and **current scalor**. As the name implies, a voltage scalor multiplies the voltage (abscissa) of each point on the $v - i$ curve by a prescribed constant k_v, while maintaining the same value of current at the same point. This requirement can be characterized by:

$$v_1 = k_v v_2 \tag{2.153}$$

$$i_1 = -i_2 \tag{2.154}$$

The negative sign in Eq. (2.154) is necessary because we want $i_1 = i$ (i.e., i is unchanged by a **voltage** scalor).

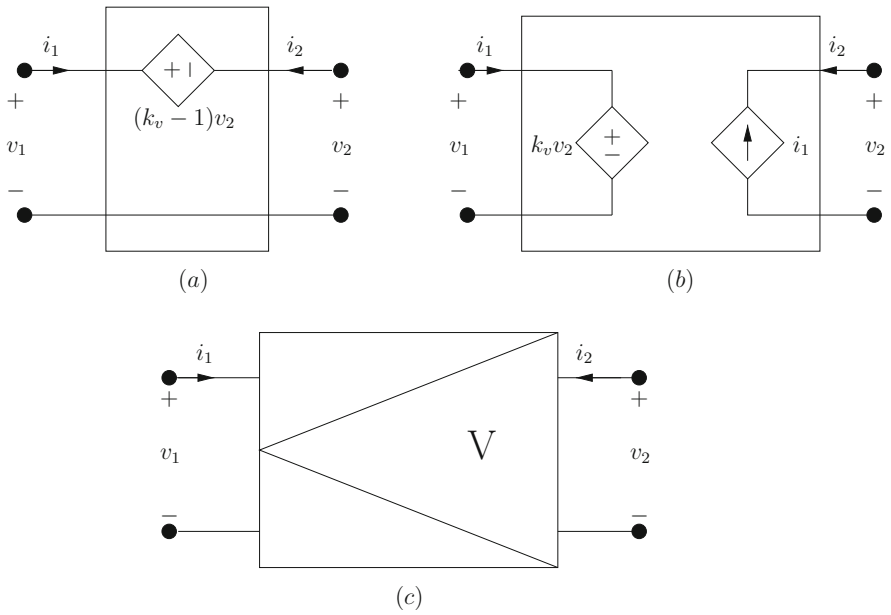

Fig. 2.43 (**a**), (**b**) Two realizations of a voltage scalor using dependent sources. (**c**) Circuit symbol

Example 2.5.10 Show that Fig. 2.43a, b realizes Eqs. (2.153) and (2.154).

Solution For (a), KVL gives:

$$\begin{aligned} v_1 &= v_2 + (k_v - 1)v_2 \\ &= k_v v_2 \end{aligned} \tag{2.155}$$

KCL applied to the dependent source gives:

$$i_1 = -i_2 \tag{2.156}$$

For (b), KVL applied to port 1 gives:

$$v_2 = k_v v_2 \tag{2.157}$$

KCL applied to port 2 gives:

$$i_1 = -i_2 \tag{2.158}$$

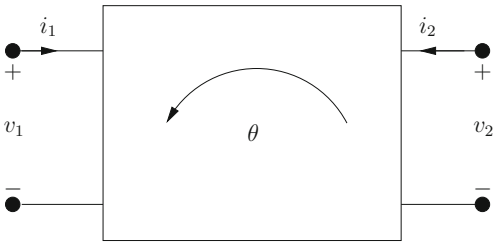

Fig. 2.44 Symbol of a rotator

It is important to realize that a scalor is completely different from the opamp scaling circuits that we discussed. The independent variable for a scalor is either a voltage or a current, whereas the independent variable for a scaling circuit is time. Since two relationships must be satisfied by a scalor, in comparison with only one for a scaling circuit, it is more difficult to realize a scalor in practice.

The dual of the voltage scalor is the current scalor, discussed in Exercise 2.8.

Now, we will discuss the rotator, whose circuit symbol is shown in Fig. 2.44. From analytic geometry, we know that the relationship required to rotate a point P with coordinates (v, i) into a point P' with coordinates (v_1, i_1) by $\theta°$ (in the counterclockwise direction) is given by:

$$\begin{pmatrix} v_1 \\ i_1 \end{pmatrix} = \begin{pmatrix} \cos\theta & -\sin\theta \\ \sin\theta & \cos\theta \end{pmatrix} \begin{pmatrix} v \\ i \end{pmatrix} \tag{2.159}$$

Example 2.5.11 Recast Eq. (2.159) in terms of port variables.

Solution From Fig. 2.42, we know that $v = v_2, i = -i_2$. Simply substituting for (v, i) in Eq. (2.159), we get the two-port relationships:

$$\begin{pmatrix} v_1 \\ i_1 \end{pmatrix} = \begin{pmatrix} \cos\theta & \sin\theta \\ \sin\theta & -\cos\theta \end{pmatrix} \begin{pmatrix} v_2 \\ i_2 \end{pmatrix} \tag{2.160}$$

In order to allow an arbitrary current scale (since physical currents are usually an order of magnitude less than voltages), we multiply i_1 and i_2 in Eq. (2.160) by a scale factor R, thereby obtaining:

$$\begin{pmatrix} v_1 \\ i_1 \end{pmatrix} = \begin{pmatrix} \cos\theta & (\sin\theta)R \\ \frac{\sin\theta}{R} & -\cos\theta \end{pmatrix} \begin{pmatrix} v_2 \\ i_2 \end{pmatrix} \tag{2.161}$$

A rotator is completely characterized by Eq. (2.161). In the volt-milliampere plane, $R = 10^3$. A physical implementation of a rotator is simply obtained by using a π-network, as Example 2.5.12 shows.

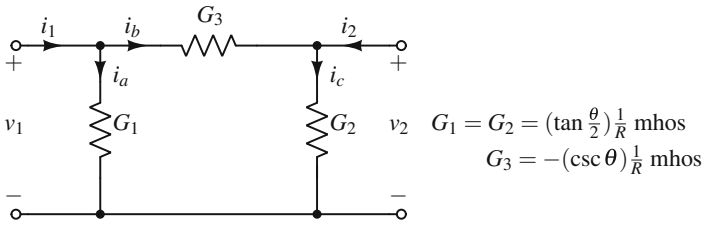

Fig. 2.45 A rotator can be implemented by choosing specific conductances G_n, given the rotation angle θ

Example 2.5.12 Show that the resistive network in Fig. 2.45 implements a rotator, given a specified angle θ.

Solution In order to verify the realization, we need only to drive v_1 and i_1 in terms of v_2 and i_2 for the network and show that they agree with Eq. (2.161).

By inspection, $i_a = G_1 v_1, i_b = G_3(v_1 - v_2), i_c = G_2 v_2$. Applying KCL to each port, we obtain:

$$i_1 = G_1 v_1 + G_3(v_1 - v_2) = \left(\tan\frac{\theta}{2}\right)\frac{1}{R}v_1 + (-\csc\theta)\frac{1}{R}(v_1 - v_2) \tag{2.162}$$

$$i_2 = G_2 v_2 - G_3(v_1 - v_2) = \left(\tan\frac{\theta}{2}\right)\frac{1}{R}v_2 - (-\csc\theta)\frac{1}{R}(v_1 - v_2) \tag{2.163}$$

With the help of the trigonometric identity: $\tan\frac{\theta}{2} = (\csc\theta - \cot\theta)$, we can simplify the above equations to:

$$i_1 = -(\cot\theta)\frac{1}{R}v_1 + (\csc\theta)\frac{1}{R}v_2 \tag{2.164}$$

$$i_2 = (\csc\theta)\frac{1}{R}v_1 - (\cot\theta)\frac{1}{R}v_2 \tag{2.165}$$

Solving Eq. (2.165) for v_1, we obtain the v_1 row in Eq. (2.161). Substituting the obtained expression for v_1 in Eq. (2.164), we obtain the i_1 row in Eq. (2.161).

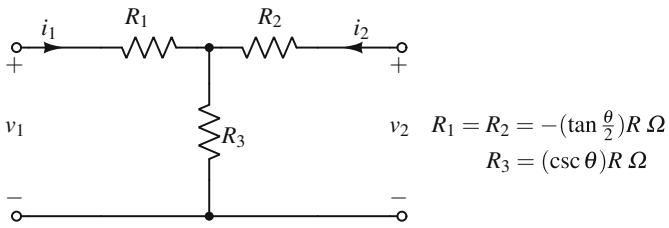

Fig. 2.46 Dual T-network for the π-network from Fig. 2.45

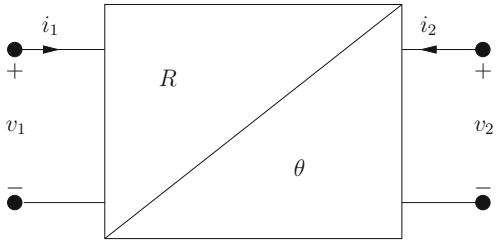

Fig. 2.47 Symbol of a reflector

Note that in the example above, since we have a π-network, we chose to work with conductances instead of resistances. That made our calculations much easier. Analogous to a π-network, we could have also worked with the T-network (recall Example 2.2.1) shown in Fig. 2.46, where working with resistances makes our calculations much simpler. Observe that, depending upon the values of θ, either one or two of the three linear resistors in both realizations may assume negative values. However, only one negative resistor is necessary to realize a rotator with any angle of rotation, provided we choose the π-network whenever $0° < \theta < 180°$, and the T-network whenever $180° < \theta < 360°$. We have already discussed how to synthesize negative resistors in Sect. 2.5.3.2.

A subset of the generic rotator is the reflector, so called because θ is the angle which the line of reflection (through the origin) makes with the horizontal axis. Hence, from analytic geometry, we obtain the characteristic two-port equations for the reflector below:

$$\begin{pmatrix} v_1 \\ i_1 \end{pmatrix} = \begin{pmatrix} \cos 2\theta & -(\sin 2\theta)R \\ \frac{\sin 2\theta}{R} & \cos 2\theta \end{pmatrix} \begin{pmatrix} v_2 \\ i_2 \end{pmatrix} \tag{2.166}$$

We shall denote a reflector by the symbol shown in Fig. 2.47. Exercise 2.9 explores reflector realizations, analogous to rotator realizations discussed previously.

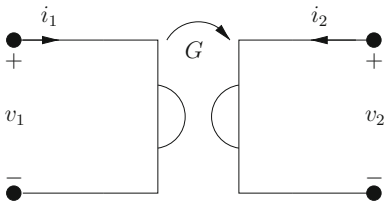

Fig. 2.48 Symbol of a gyrator

2.5.4.2 Gyrators

There are several angles of reflection which are of special practical importance, and the corresponding reflectors have been given special names. We will discuss a particularly important kind, called a gyrator (for other specific reflectors, please refer to [3]).

When $\theta = 45°$, Eq. (2.166) can be recast into the form:

$$\begin{pmatrix} i_1 \\ i_2 \end{pmatrix} = \begin{pmatrix} 0 & G \\ -G & 0 \end{pmatrix} \begin{pmatrix} v_1 \\ v_2 \end{pmatrix} \tag{2.167}$$

where $G = \frac{1}{R}$ is a constant called the **gyration conductance**. The symbol for a gyrator is shown in Fig. 2.48. The fundamental property of an ideal gyrator is that it functions as an "impedance inverter." For instance, if the output port (port 2) of the gyrator is terminated with an $R_L - \Omega$ linear resistor, the input port's resistance is given by:

$$\begin{aligned} \frac{v_1}{i_1} &= \frac{-i_2/G}{Gv_2} \\ &= \frac{1}{G^2}\frac{-i_2}{v_2} \\ &= \frac{G_L}{G^2} \end{aligned} \tag{2.168}$$

In other words, $R_1 = \frac{G_L}{G^2}$. If $G = 1$, we see that the input port's resistance is the **reciprocal** of the output port's resistance. Hence the term "impedance inverter."

The specification definition of "impedance" as a "frequency-dependent resistance" will become clear in Sect. 4.3. Specifically, we will discuss that if the output port of an ideal gyrator is terminated with a capacitor, the input port behaves like an inductor. Thus, a gyrator is a useful element in the design of inductorless filters. This is practically advantageous because physical inductors tend to be bulky and lossy, when compared to physical capacitors. We will see such an implementation in the exercises to Chap. 4.

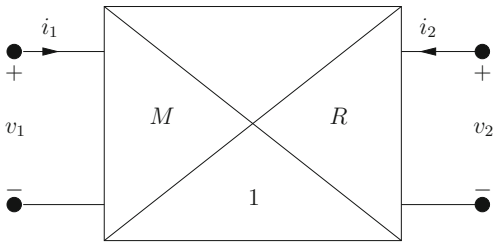

Fig. 2.49 Symbol for a Type 1 $M - R$ mutator

2.5.4.3 Mutators

So far, we have discussed two-port resistors which share the common property that each transforms a nonlinear resistor into another nonlinear resistor. If we liken the four basic network elements, resistors, capacitors, inductors, and memristors, to four distinct species in the generic sense, then the scalor, rotator, and reflector can be said to transform elements belonging to the same species.

In this section, we will show that it is possible to produce a **mutation** from one species into another with the help of a two-port black box called the **mutator**. For example, it is possible to connect a resistor across port 2 of a mutator and produce an inductor across port 1. Conversely, if an inductor is connected across port 1 of the same mutator, a resistor is produced across port 2. For this reason, this class of mutators is called $L - R$ **mutators**.[11]

In the interest of brevity,[12] and the fact that very few physical electronic memristors are commercially available, we will devote this section to the design of $M - R$ mutators for realizing memristors from nonlinear resistors [1]. We chose nonlinear resistors because they can be more easily synthesized and are even commercially available (for example, diodes), as opposed to nonlinear capacitors or inductors.

Figure 2.49 shows the circuit symbol of a Type 1 $M - R$ mutator. In order to transform a resistor into a memristor, it is necessary that the coordinates (v, i) of each point on a $v - i$ curve be transformed into a corresponding point with coordinates (ϕ, q). To accomplish this, first recall the following relationships from our two-port black box in Fig. 2.42: $v_2 = v, i_2 = -i$. Suppose:

$$v_1 \triangleq k_v \frac{dv_2}{dt} \tag{2.169}$$

$$i_1 \triangleq k_i \left(-\frac{di_2}{dt} \right) \tag{2.170}$$

[11] We want to clarify mutator terminology. In Chua's seminal book "Introduction to Nonlinear Circuit Theory" [3], Dr. Chua refers to an $L - R$ mutator as an $R - L$ mutator. However, in Dr. Chua's publication defining the mutator [2] and all subsequent works, the terminology is consistent with the one used in this book.

[12] For details on realizing other types of mutators such as $C - R$, $R - L$, etc., please refer to [2].

k_v and k_i are constants that are used for dimensional consistency. We will see in Sect. 2.5.5 when we realize an $M-R$ mutator as to how to compute these constants. Using the definitions in Eqs. (2.169) and (2.170), we have at port 1:

$$\begin{aligned}\phi_1 &\triangleq \int_{-\infty}^{t} v_1(\tau)d\tau \\ &= k_v \int_{-\infty}^{t} \frac{d}{d\tau} v_2(\tau)d\tau \\ &= k_v \int_{-\infty}^{t} \frac{d}{d\tau} v(\tau)d\tau \\ &= k_v v \end{aligned} \tag{2.171}$$

Similarly:

$$\begin{aligned}q_1 &\triangleq \int_{-\infty}^{t} i_1(\tau)d\tau \\ &= k_i \int_{-\infty}^{t} \frac{-d}{d\tau} i_2(\tau)d\tau \\ &= k_i \int_{-\infty}^{t} \frac{d}{d\tau} i(\tau)d\tau \\ &= k_i i \end{aligned} \tag{2.172}$$

Thus, our mutator does perform the correct mapping. A high-level realization of a Type 1 $M-R$ mutator using dependent sources is shown in Fig. 2.50.

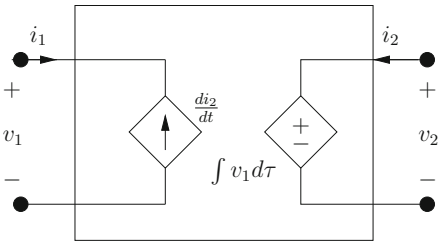

Fig. 2.50 One realization of an $M-R$ mutator, $k_v = 1$, $k_i = 1$. For other $M-R$ mutators such as Type 2, please refer to [1]

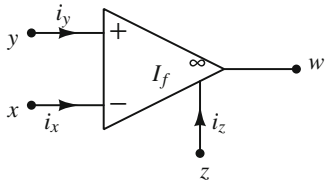

Fig. 2.51 An ideal CFOA. Labels that are prevalent in the literature: output terminal is labeled w, the inverting input is labeled x, noninverting input is labeled y, and the compensation terminal (pin) is labeled z

2.5.5 Current Feedback Opamps

So far, in this section, we have been using opamps that rely on voltage feedback. There is another kind of opamp that uses **current feedback**, appropriately named **current feedback operational amplifier (CFOA)**.

A CFOA is a four-terminal[13] device [10] with the circuit symbol[14] shown in Fig. 2.51.

The terminal behavior of an ideal CFOA is defined below:

$$i_x = i_z \tag{2.173}$$

$$i_y = 0 \tag{2.174}$$

$$v_x - v_y = 0 \tag{2.175}$$

$$v_w - v_z = 0 \tag{2.176}$$

Note that the current through the compensation pin i_z is feedback to the inverting input current i_x, hence the origin of the name "CFOA."

A CFOA is particularly suited for implementing derivative (or integral) operations in controlled sources. Hence, we can easily realize two-ports such as the Type 1 $M - R$ mutator from Fig. 2.50, as the following example shows.

[13]Some CFOAs do not have an externally accessible compensation pin z, to maintain pin-compatibility with voltage feedback amplifiers. However, such devices are actually a special class of CFOAs and in this book we will use only the very general CFOAs such as the AD844 that have an externally accessible compensation pin. We will henceforth refer to such CFOAs as an **ideal CFOA**.

[14]A literature search revealed that there is no standard symbol for a CFOA. We are defining this symbol because it closely mimics the symbol of an ideal opamp with the I_f clarifying that we have current feedback.

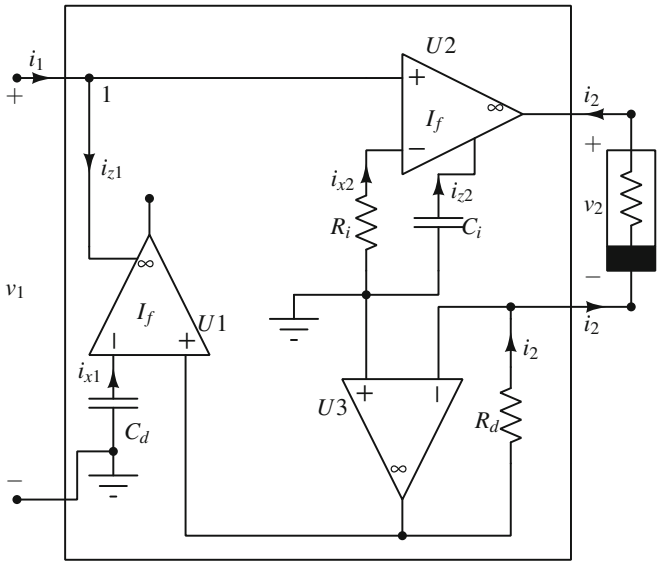

Fig. 2.52 Type 1 $M-R$ mutator realization [1]

Example 2.5.13 Show that the network in Fig. 2.52 implements a Type 1 $M-R$ mutator.

Solution First, we will derive Eq. (2.169): $v_1 = k_v \frac{dv_2}{dt}$. For CFOA $U2$, we have the voltage across C_i equal to v_2. Notice that this is possible because the inverting terminal of opamp $U3$ is at virtual ground. Thus:

$$i_{z2} = -C_i \frac{dv_2}{dt} \tag{2.177}$$

Also, for CFOA $U2$:

$$i_{x2} = i_{z2} \tag{2.178}$$

$$v_1 = v_{x2} \tag{2.179}$$

Using Ohm's law for R_i and simplifying using the above equations:

$$\begin{aligned} v_1 &= -i_{x2} R_i \\ &= -i_{z2} R_i \end{aligned}$$

(continued)

Example 2.5.13 (continued)

$$= R_i C_i \frac{dv_2}{dt} \tag{2.180}$$

Hence, $v_1 = k_v \frac{dv_2}{dt}$, where $k_v = R_i C_i$. For deriving Eq. (2.170): $i_1 = k_i \left(-\frac{di_2}{dt}\right)$, application of KCL at node 1 gives $i_1 = i_{z1}$ (since current into the noninverting input of CFOA $U2$ is zero). From CFOA $U1$:

$$i_{x1} = i_{z1} \tag{2.181}$$

From capacitor C_d:

$$i_{x1} = -C_d \frac{dv_{x1}}{dt} \tag{2.182}$$

Note that output voltage of opamp $U3$ is $R_d i_2$, which is equal to v_{y1}. But, since $v_{x1} = v_{y1}$, we get:

$$v_{x1} = R_d i_2 \tag{2.183}$$

Substituting for v_{x1} in the expression for i_{x1}, and using the fact that $i_{x1} = i_{z1} = i_1$, we get:

$$i_1 = -R_d C_d \frac{di_2}{dt} \tag{2.184}$$

Hence, $i_1 = k_i \frac{di_2}{dt}$, where $k_i = R_d C_d$.

Further detailed discussion of CFOAs is beyond the scope of this book, but the interested reader should consult excellent references such as [10].

2.6 Conclusion

This chapter greatly expanded upon Chap. 1 and we should now have a very good understanding of the laws of elements, for a variety of multi-terminal elements. To summarize:

1. To characterize a multi-terminal black box, we will choose one node as ground (reference). We can then classify the black box as either an n-terminal resistor (involving $n-1$ terminal voltages and currents), an n-terminal inductor (involving $n-1$ terminal currents and flux-linkages), an n-terminal capacitor (involving

$n-1$ terminal voltages and charges), and an n-terminal memristor (involving $n-1$ terminal flux-linkages and charges).
2. Since most practical devices have single digit values for n (the number of terminals), we can characterize three-terminal ($n=3$) resistors, inductor, capacitors, and memristors using the six two-port representations: current-controlled, voltage-controlled, hybrid 1, hybrid 2, transmission 1, and transmission 2.
3. We studied the four dependent sources: CCVS, VCCS, CCCS, and VCVS and transformers as linear resistive two-ports.
4. We studied the *npn* BJT as a nonlinear resistive two-port.
5. A common three-terminal inductor is the physical transformer, usually consisting of two coupled coils wound on a torus of ferromagnetic material.
6. A particularly useful multi-terminal element for redistributing power is the three-port circulator.
7. The opamp is a very versatile multi-terminal nonlinear resistor. We implemented amplifiers and studied nonlinear opamp circuits such as the Schmitt trigger and NICs.
8. The family of two-port resistors: scalors, rotators, reflectors, along with the mutator can be realized using dependent sources. For the mutator, we used a CFOA.

We are now ready to learn about the laws of interconnections, starting with resistive nonlinear networks in Chap. 3.

Exercises

2.1 For the linear two-ports specified by the following equations, find as many representations as you can.

1. $$\begin{aligned} -i_1 + 2i_2 + v_2 &= 0 \\ v_1 + v_2 &= 0 \end{aligned}$$
2. $$\begin{aligned} v_1 + i_2 + v_2 &= 0 \\ i_1 &= 0 \end{aligned}$$
3. $$\begin{aligned} v_1 + v_2 &= 0 \\ i_1 + i_2 &= 0 \end{aligned}$$

2.2 By equating the inductance matrix in Eq. (2.65) (from Example 2.2.5) to the matrix from Eq. (2.55), show that:

$$n = \frac{L_{22}}{M} \qquad L_m = \frac{M^2}{L_{22}} \qquad L_a = L_{11} - \frac{M^2}{L_{22}} \tag{2.185}$$

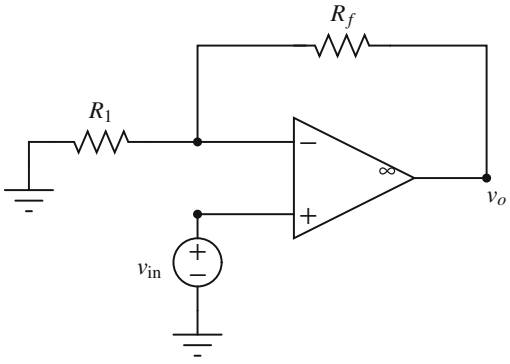

Fig. 2.53 Circuit for problem 2.3

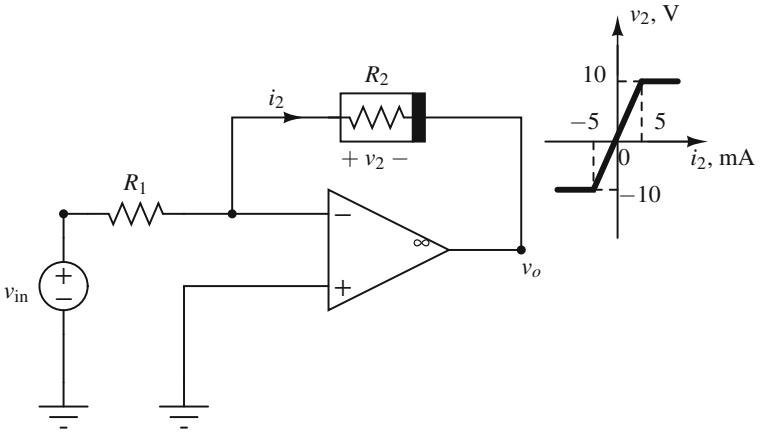

Fig. 2.54 Circuit for problem 2.4

2.3 For the inverting amplifier shown in Fig. 2.53, determine the VTC and also the dynamic range of v_{in} for which the opamp operates in the linear region.

2.4 Consider the circuit in Fig. 2.54, with the nonlinear resistor's DP shown.

1. Compute the nonlinear VTC v_o-vs-v_{in}.
2. Determine the dynamic range for v_{in}, for which the opamp remains in the linear region.
3. Does the opamp operate in the linear region for **all** values of v_{in}, in spite of a nonlinear element in the feedback path? Justify your answer.

2.5 Consider the VTC of the **finite gain opamp model** shown in Fig. 2.55. Using the PWL representation (Eq. (1.52) from Sect. 1.9.1.2), we can describe the finite

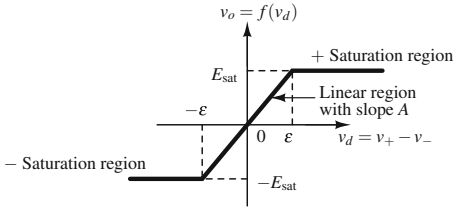

Fig. 2.55 VTC for problem 2.5

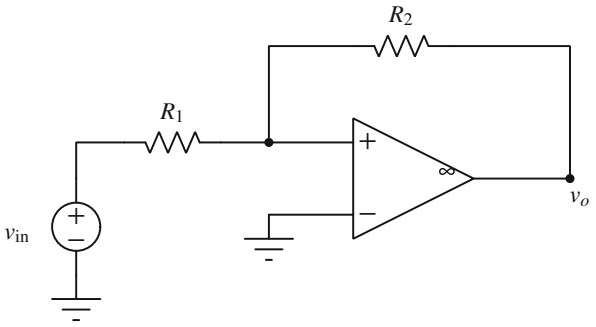

Fig. 2.56 Circuit for problem 2.6

gain model analytically as shown below:

$$i_- = 0 \tag{2.186}$$

$$i_+ = 0 \tag{2.187}$$

$$v_o = \frac{A}{2}|v_d + \epsilon| - \frac{A}{2}|v_d - \epsilon| \tag{2.188}$$

1. Derive circuits similar to Fig. 2.28b, c, and d for the finite gain opamp model. HINT: For the linear region, you will require a VCVS.
2. Now, re-derive the VTC for the inverting amplifier from Example 2.5.4 using the finite gain model.
3. Confirm that as $A \to \infty$ in your finite gain VTC, we obtain Eq. (2.105).

2.6 Derive the VTC and validating inequalities for the noninverting Schmitt trigger in Fig. 2.56. Also, sketch the VTC.

2.7 Experimentally plot the DP characteristic for Fig. 2.41a. Determine the percent error between the experimental measurements and theoretical calculations for the slopes and breakpoints given by Eqs. (2.148), (2.151), and (2.152).

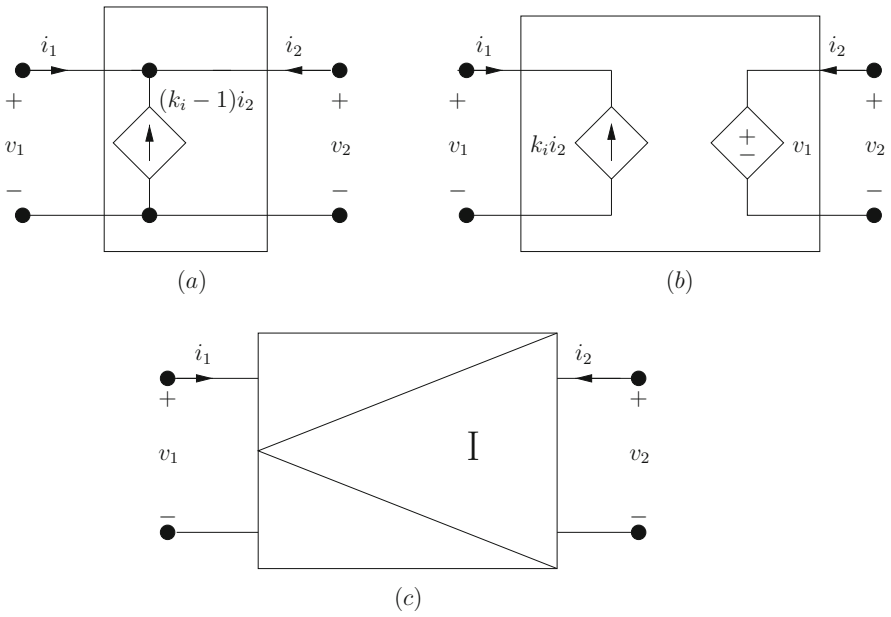

Fig. 2.57 For problem 2.8: (**a**) dependent source implementation 1, (**b**) dependent source implementation 2, (**c**) scalor

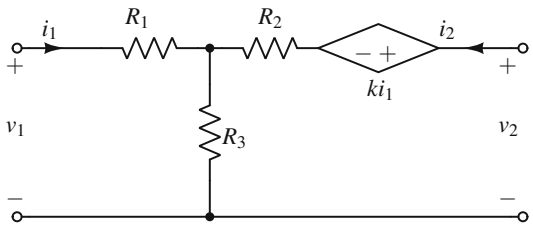

$R_1 = (\cot\theta)R\ \Omega$
$R_2 = (\tan\theta)R\ \Omega$
$R_3 = -(\csc 2\theta)R\ \Omega$
$k = 2(\csc 2\theta)R\ \Omega$

Fig. 2.58 Circuit for problem 2.9

2.8 Derive the following current scalor relationships for the dependent source implementations in Fig. 2.57a, b:

$$v_1 = v_2 \tag{2.189}$$

$$i_1 = -k_i i_2 \tag{2.190}$$

2.9 Show that the circuit in Fig. 2.58 realizes the reflector two-port model in Eq. (2.166).

Lab 2: Noninverting Schmitt Trigger VTC

Objective: To verify the Schmitt trigger characteristics from Exercise 2.6 via QUCS simulation and physical implementation

Theory:

You may be wondering if one can actually physically observe the VTCs for the Schmitt triggers. The answer is yes. In order to do this, consider the circuit shown in Fig. 2.59. We have used the circuit symbol for the finite gain opamp model. Nevertheless, for this lab, we can assume that the opamps are ideal.

The capacitor C_f and resistor R_b provide feedback at higher frequencies (for eliminating instability due to parasitics) and can be ignored for very low frequencies. In fact, at DC ("zero" frequency), the capacitor acts like an open circuit (more on this in Chap. 4) and since the current into the inverting terminal of an opamp is zero, we get Fig. 2.60, that we will use for analysis.

Lab Exercise:

1. First, for the purposes of this lab, we can assume that the upper opamp is operating in the linear region. In fact, you should recognize the upper opamp as a variant of the summing amplifier from Example 2.5.5.

   Using KCL at the inverting input of the upper opamp, write an equation in terms of **conductances** G_u, G_H, G_v and voltages u, v_{out}, v_{in}.

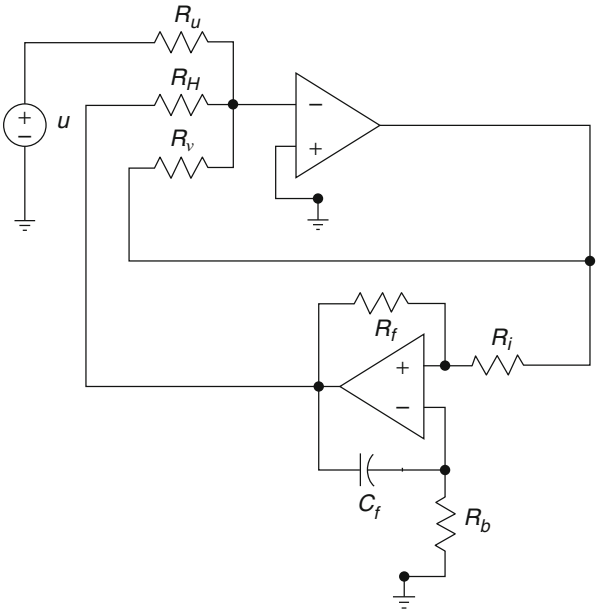

Fig. 2.59 Schematic for experimentally confirming the Schmitt trigger VTC

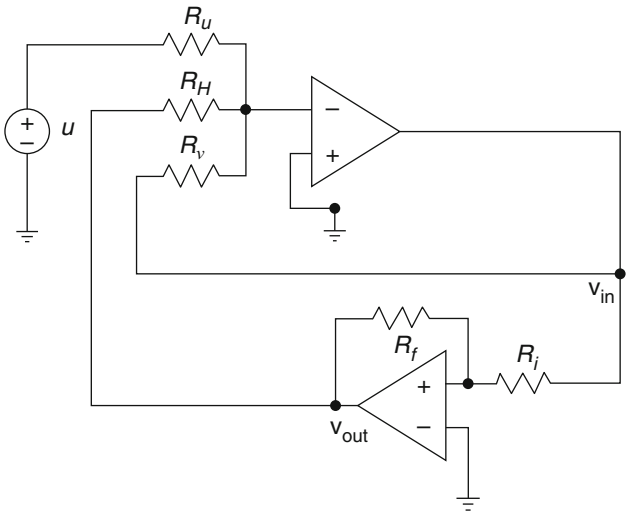

Fig. 2.60 Schematic for analysis

2. Assuming $G_u = G_H = G_v$, find the constraint imposed by the summing amplifier.
3. This step should help you understand the elegant mathematical trick: the constraint that you get from the previous step is essentially shown in Fig. 2.61a, b

   In other words, the derived constraint in step 2 implies that the circuit is **intersecting** the line $v_{\text{out}} = -(v_{\text{in}} + u)$ with the VTC of the Schmitt trigger. This intersection is the elegant mathematical trick: obviously, only one of the two Fig. 2.61a, b will occur in reality.

   Before proceeding to the simulation and experimental verification, component values that we used are: $R_f = 20\,\text{k}\Omega$, $R_i = 10\,\text{k}\Omega$, $R_u = R_H = R_v = 20\,\text{k}\Omega$, $R_b = 470\,\Omega$, $C_f = 470\,\text{pF}$. Opamps are TL074, we chose power supply voltages such that $E_{\text{sat}} = \pm 4\,\text{V}$. u was varied using a sine function with an amplitude of 8 V. Maximum frequency used was 100 Hz.
4. Use QUCS to confirm the VTC of the noninverting Schmitt trigger by using the schematic in Fig. 2.59.
5. Physically implement your circuit from Fig. 2.59 and experimentally confirm the noninverting Schmitt trigger VTC. Our result is shown in Fig. 2.62. The reference for this lab is [8]. We highly recommend going through Kennedy and Chua's seminal work, if you have access to it. It very clearly dispels common misconceptions about the nature of hysteresis in electronic circuits.

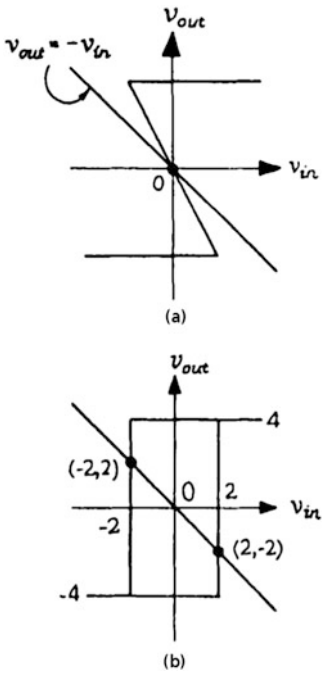

Fig. 2.61 The result of intersecting the line $v_{\text{out}} = -(v_{\text{in}} + u)$ with the VTC of the Schmitt trigger will result in either (**a**) or (**b**). Note that we have used $u = 0$ in this figure

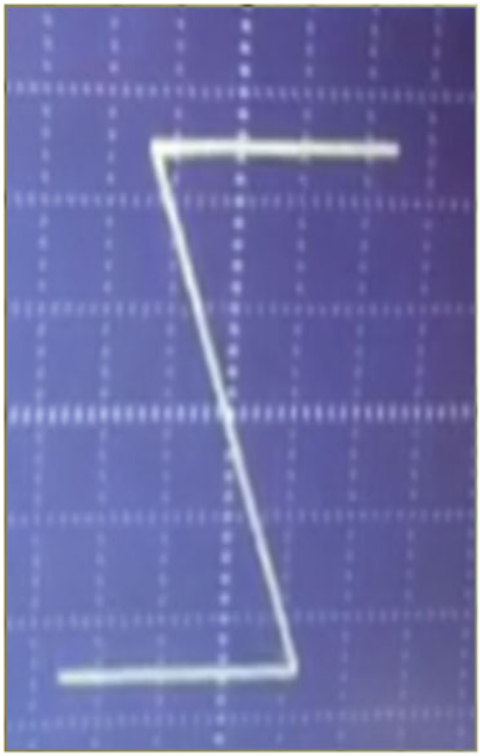

Fig. 2.62 Experimental confirmation of Schmitt trigger VTC

References

1. Biolek, D. et al.: Mutators for transforming nonlinear resistor into memristor. In: 20th European Conference on Circuit Theory and Design (ECCTD), pp. 488–491 (2011)
2. Chua, L.O.: Synthesis of new nonlinear network elements. Proc. IEEE **56**(8), 1325–1342 (1968)
3. Chua, L.O.: Introduction to Nonlinear Network Theory. McGraw-Hill, New York, (1969), (out of print)
4. Chua, L.O.: University of California, Berkeley EE100 Fall 2008 Supplementary Lecture Notes. (2008) Multi-Terminal Resistors: http://inst.eecs.berkeley.edu/~ee100/fa08/lectures/EE100supplementary_notes_4.pdf. Opamps: http://inst.eecs.berkeley.edu/~ee100/fa08/lectures/EE100supplementary_notes_7.pdf. Accessed 12 April 2017
5. Chua, L.O., Ayrom F.: Designing nonlinear single op-amp circuits: a cookbook approach. Int. J. Circuit Theory Appl. **13**, 235–268 (1985)
6. Chua, L.O., Desoer, C.A., Kuh, E.S.: Linear and Nonlinear Circuits. McGraw-Hill, New York (1987), (out of print)
7. Howe, R.T., Sodini, J.T.: Microelectronics: An Integrated Approach. Prentice-Hall, Upper Saddle River (1996)

8. Kennedy, M.P., Chua, L.O.: Hysteresis in electronic circuits: a circuit theorist's perspective. Int. J. Circuit Theory Appl. **19**, 471–515 (1991)
9. Ranganathan, S., Tsividis, Y.: Discrete-time parametric amplification based on three-terminal MOS varactor: analysis and experimental results. IEEE J. Solid-State Circuits **38**(12), 2087–2093 (2003)
10. Senani, R. et al.: Current Feedback Operational Amplifiers and Their Applications. Springer, Berlin (2013)